Sensor and Simulation Notes

Note 163

January 1973

Performance of an Admittance Sheet Plus Coplanar Flanges as a Matched
Termination of a Two-Dimensional Parallel-Plate Transmission Line
I. Perpendicular Case

by

A. D. Varvatsis and M. I. Sancer
Northrop Corporate Laboratories
Pasadena, California

Abstract

The reflections of a monochromatic TEM wave or a step-function TEM pulse
from an R,L admittance sheet terminating the transmission line are calculated.
To minimize these reflections the value of R can be determined by a low-
frequency argument whereas the choice of the optimum L requires a parametric
study for various values of L. Parametric plots are presented of the reflected
field components in both the frequency and time domains that allow the
determination of the optimum values for L. It is found that a suitable choice
of L can considerably minimize reflections.

I. Introduction and Results

The concept of an admittance sheet as a distributed termination for a TEM transmission line was introduced in ref. 1. A subsequent note [2] considered a sloped R,L admittance sheet as a matched termination for a two-dimensional parallel-plate transmission line with coplanar conducting flanges. The resistance R was calculated by a low-frequency argument, whereas the optimum L to match the transmission line for an incident TEM step pulse, was chosen on the basis of an approximate method involving a comparison of the current induced on a perfect termination (zero reflection) to the approximate current induced on the admittance sheet. The resulting R,L admittance sheet does not provide a perfect termination, and consequently it causes a reflection of the incident TEM wave. A quantitative calculation of the reflected field would allow the evaluation of the performance of the admittance sheet in both the frequency and time domains.

In this note we consider a two-dimensional parallel-plate transmission line with coplanar conducting flanges, to facilitate the mathematical analysis, terminated by an R,L admittance sheet. We calculate the reflection of a TEM monochromatic wave and a TEM unit step pulse for the special case of a perpendicular admittance sheet only. The value of the resistance R is taken from ref. 2 whereas a parametric study for various L will determine the optimum inductance corresponding to minimum reflection. Our method involves the derivation of an integral equation for the aperture electric field in the frequency domain, and is based on the application of the boundary condition across the admittance sheet coupled with two integral relationships for the interior and exterior magnetic fields in terms of the aperture electric field. The reflected TEM mode and the first four TM modes are calculated in both the frequency and time domain. In the time domain the reflected TM modes decay considerably with distance and consequently it is important that the reflected TEM pulse should be minimized to make a suitable choice for the inductance L. This value of L is approximately equal to $1.1 \, (hZ_o/c)$, where h is the height, $Z_o = 377\Omega$ and c is the speed of light. The value of L obtained in ref. 2 is very close to ours. The maximum TEM reflection coefficient for the above choice of L is only 3.2%. In the frequency domain the optimum L to minimize the TEM reflection over the entire spectrum is approximately the same as in the time domain and the

2

maximum absolute value of the reflection coefficient is 3.5%. However, for a given frequency the value of L depends on this frequency. The reflection for the TM modes is minimized when the inductance is zero. In the frequency domain the corresponding maximum absolute values for the reflection coefficients of the transverse electric field component are 14%, 7%, 4.5% and 3.4% for the first four modes respectively. For the case of zero inductance the maximum TEM reflection coefficient is equal to -1/3 at infinite frequency or at t = 0+. If the incident TEM wave is monochromatic with a frequency below cutoff for all the TM modes, then the reflected TM modes will be evanescent and the choice of L is made by minimizing the TEM reflection. This value of L depends on the frequency of the TEM wave. However, if the frequency of the incident TEM wave is above cutoff for the first or higher TM modes, then one or more of the reflected TM modes will propagate and the choice of L cannot be made on the basis of minimizing the TEM mode only. Plots are given of the reflection coefficients (for the transverse electric field component) of the TEM and the first four TM modes versus frequency, with L as a parameter (see Figs. 5 through 9). From these plots one can choose the value of L that will minimize the overall reflection if some of the TM modes are propagating. Notice, however, that for high frequencies all the propagating TM modes become negligibly small irrespective of the value of L, and the choice of L should be made by minimizing the TEM reflection. This is also true, as we mentioned earlier, for frequencies below cutoff.

For a detailed description of the plots of the field components which allow the evaluation of the optimum L see section IV.

II. Formulation of the Problem

Consider a two-dimensional parallel-plate transmission line terminated by a sloped R,L admittance sheet, where R and L are independent of the frequency. To facilitate the mathematical analysis two metallic flanges of infinite extent coplanar to the termination plane have been added (Fig. 1). The purpose of this note is to calculate and minimize the reflection of an incident TEM wave by suitably choosing R and L. A low-frequency or equivalently a late-time argument can be invoked to determine the value of R [2]. Thus

$$R = Z_o \sin \xi \tag{1}$$

where Z_o is the free-space characteristic impedance. A parametric study for various L will be made to determine the optimum value for the inductance L.

Consider now a monochromatic TEM wave $\underline{E}^{inc} = e^{ik_o z} \hat{e}_x$ travelling down the transmission line. The reflected wave will consist of a TEM (E_x, H_y) and TM (E_x, H_y, E_z) modes. The fields are independent of the y coordinate and the following relationships hold:

$$E_x = e^{ik_o z} + \Gamma e^{-ik_o z} + \sum_{n=1}^{\infty} C_n \cos(2n\pi x/h) e^{-i\gamma_n z} \tag{2}$$

$$H_y = (1/Z_o) e^{ik_o z} - (\Gamma/Z_o) e^{-ik_o z} - \sum_{n=1}^{\infty} (C_n/Z_n) \cos(2n\pi x/h) e^{-i\gamma_n z} \tag{3}$$

$$E_z = \sum_{n=1}^{\infty} i(2n\pi/\gamma_n h) C_n \sin(2n\pi x/h) e^{-i\gamma_n z} \tag{4}$$

where Γ and C_n's are coefficients to be determined, $k_o = \omega/c$, $Z_n = \gamma_n/\omega\varepsilon_o$, and γ_n is defined by the relationship

$$\gamma_n^2 = k_o^2 - (2n\pi/h)^2$$

with $\gamma_n = [k_o^2 - (2n\pi/h)^2]^{\frac{1}{2}}$ for $k_o > 2n\pi/h$, $\gamma_n = i[(2n\pi/h)^2 - k_o^2]^{\frac{1}{2}}$ for $k_o < 2n\pi/h$ to ensure evanescent reflected waves ($z < 0$). The symbol $(a)^{\frac{1}{2}}$ for $a > 0$ is the

4

positive square root of a. Equations (2), (3) and (4) hold in the region.
$z < -(\tfrac{1}{2})h \cot \xi$.

To solve our problem we first cast the boundary conditions in a suitable
form. The boundary conditions are:

$$E_z = 0 \quad \text{on the plates} \tag{5}$$

$$E_s = 0 \quad \text{on the flanges} \tag{6}$$

If we use Maxwell's equation $\nabla \times \underline{H} = -i\omega\varepsilon_o \underline{E}$ we obtain

$$\frac{\partial H_y}{\partial x} = -i\omega\varepsilon_o E_z \tag{7}$$

$$-\frac{\partial H_y}{\partial z} = -i\omega\varepsilon_o E_x \tag{8}$$

From (7) and (8) we can deduce that

$$\frac{\partial H_y}{\partial n} = \nabla H_y \cdot n = \frac{\partial H_y}{\partial x} \cos \xi + \frac{\partial H_y}{\partial x} \sin \xi$$

$$= -i\omega\varepsilon_o (\cos \xi \, E_z - \sin \xi E_x)$$

$$\frac{\partial H_y}{\partial n} = -i\omega\varepsilon_o (\underline{E} \cdot \hat{s}) = -i\omega\varepsilon_o E_s \tag{9}$$

and the boundary conditions (5) and (6) become

$$\frac{\partial H_y}{\partial x} = 0 \quad \text{on the plates} \tag{10}$$

$$\frac{\partial H_y}{\partial n} = 0 \quad \text{on the flanges} \tag{11}$$

It is easy to verify that H_y satisfies

$$\left(\frac{\partial^2}{\partial x^2} + \frac{\partial^2}{\partial z^2}\right) H_y = 0 \tag{12}$$

5

in both regions I and II (Fig. 2). To derive suitable integral relationships, for the magnetic and electric fields, that can lead to integral equations of the aperture fields we use Green's theorem for both regions I and II (Fig. 2) and the boundary conditions (10), (11) to obtain

$$\int_2^1 \left(\frac{\partial G_I}{\partial n} H_{Iy} - \frac{\partial H_{Iy}}{\partial n} G_I \right) ds_1 = H_{Iy} - H_o \tag{13}$$

$$- \int_1^2 \frac{\partial H_{IIy}}{\partial n_1} G_{II} ds = H_{IIy} \tag{14}$$

where both Green's functions G_I and G_{II} satisfy

$$\left(\frac{\partial^2}{\partial x^2} + \frac{\partial^2}{\partial z^2} \right) G = \delta(x - x')\delta(z - z') \tag{15}$$

and

$$\frac{\partial G_I}{\partial x} = 0 \quad \text{on the plates} \tag{16}$$

$$\frac{\partial G_{II}}{\partial n} = 0 \quad \text{on the termination plane} \tag{17}$$

With G_I defined by (15) and (16), H_o is the incident TEM magnetic field. The radiation condition in region II makes the integral at infinity vanish. Recalling (9), equations (13) and (14) become

$$\int_2^1 \left(\frac{\partial G_I}{\partial n} H_{Iy} + i\omega\epsilon_o E_s \right) ds_1 = H_{Iy} - H_o \tag{18}$$

$$- \int_2^1 i\omega\epsilon_o E_s ds_1 = H_{IIy} \tag{19}$$

In this note we examine the vertical case ($\xi = \pi/2$) only (Fig. 3), therefore we can rewrite (18) and (19) as

$$H_{Iy}(x,z) = H_o - \int_{-h/2}^{h/2} \left(i\omega\epsilon_o E_x G_I - \frac{\partial G_I}{\partial z'} H_{Iy} \right) dx' \tag{20}$$

6

$$H_{IIy}(y,z) = \int_{-h/2}^{h/2} i\omega\varepsilon_o E_x G_{II} dx' \tag{21}$$

For the vertical case it is easy to calculate G_I with the additional boundary condition

$$\frac{\partial G_I}{\partial z'} = 0 \quad \text{on the termination plane} \tag{22}$$

and (20) can be simplified considerably. We will denote this Green's function as G_I'

$$H_{Iy} = H_o - \int_{-h/2}^{h/2} i\omega\varepsilon_o E_x G_I' dx' \tag{23}$$

The choice of G_I' subject to (22) changes the meaning of H_o. It is no longer the incident magnetic field $(1/Z_o)\exp(ik_o z)$. Instead, H_o is equal to $H^{inc} = (1/Z_o)\exp(ik_o z)$ plus the reflected field if the transmission line is short-circuited, i.e.,

$$H_o = (1/Z_o)(e^{ik_o z} + e^{-ik_o z}) \tag{24}$$

We are now in a position to derive an integral equation for the aperture electric field E_x by combining (21), (23) evaluated at $z = 0$, with the boundary condition

$$Z(\hat{n}_1 \times \underline{H}_I + \hat{n} \times \underline{H}_{II}) = \underline{E} \tag{25}$$

where $Z = R - i\omega L$ is the terminating impedance. The nature of the singularities of G_I and G_{II} is such that (21) and (23) retain their form even at $z = 0$. Had we used (20), the presence of the derivative $(\partial G_I/\partial z')$ would have produced the familiar form

$$(\tfrac{1}{2})H_{Iy}(x,z=0) = (1/Z_o) - \int_{-h/2}^{h/2} (i\omega\varepsilon_o E_x G_I - \frac{\partial G_I}{\partial z'} H_{Iy}) dx' \tag{26}$$

Noting that $\hat{n} = -\hat{n}_1 = \hat{e}_z$, (25) can be rewritten as

$$E_x = Z(H_{Iy} - H_{IIy}) \tag{27}$$

Combining (21), (23), (24) and (27) we obtain an integral equation for the aperture electric field E_x

$$E_x(x,z=0) = 2(Z/Z_o) - \int_{-h/2}^{h/2} i\omega\epsilon_o Z[G_I'(x,0;x',0) + G_{II}(x,0;x',0)]E_x(x',0)dx' \tag{28}$$

where $G_{II}(x,0;x',0) = -(i/2)H_o^{(1)}(k_o|x-x'|)$ and $H_o^{(1)}(u)$ is the Hankel function of the first kind. If we apply equation (2) at $z = 0$ we can write E_x as

$$E_x(x,0) = 1 + \Gamma + \sum_{n=1}^{\infty} C_n \cos(2n\pi x/h) = \sum_{n=0}^{\infty} C_n \cos(2n\pi x/h) \tag{29}$$

where $C_o = 1 + \Gamma$. In view of the form of (29) it is advisable to use an expression for G_I that contains trigonometric functions. If G_I only satisfies the wave equation (15) and $\partial G_I/\partial x = 0$ on the plates one can easily obtain

$$G_I = (1/2ik_oh)e^{ik_o|z-z'|} + \sum_{n=1}^{\infty} (1/i\gamma_nh)\cos(2n\pi x/h)\cos(2n\pi x'/h)e^{i\gamma_n|z-z'|} \tag{30}$$

Notice that the derivation of (30) uses the entire region $-\infty < z,z' < \infty$, $-h/2 \leq x,x' \leq h/2$ whereas its usage in the present note is restricted in region $z,z' \leq 0$, $-h/2 \leq x,x' \leq h/2$. This is legitimate since both (15) and (16) are satisfied by (30) in the desired region $z,z' \leq 0$, $-h/2 \leq x,x' \leq h/2$. (See also appendices I and V.) Using (30) we can simply construct G_I' as

$$G_I'(x,z;x',z') = G_I(x,z;x',z') + G_I(x,z;x',-z') \tag{31}$$

This form secures that $\partial G_I'/\partial z' = 0$ at $z' = 0$ which is needed to derive (23). Thus G_I' in (23) has the form ($z' = 0 > z$)

$$G_I' = (1/ik_oh)e^{-ik_oz} + \sum_{n=1}^{\infty} (2/i\gamma_nh)\cos(2n\pi x/h)\cos(2n\pi x'/h)e^{-i\gamma_nz} \tag{32}$$

To obtain G_I' in (28) we simply set $z = 0$ in (32). One can verify that if (29) and (32) are substituted in (23) the resulting form for $H_{Iy}(x,z)$ is the one given by equation (3). (See appendix I.) It is also interesting to notice that

8

if (26) were used instead of (23) one could still derive integral equation (28). This point is examined in appendix II. Using (29) and (32) evaluated at $z = 0$, we can cast (28) into an infinite system of algebraic equations with the C_n's as unknowns. This can be done in two steps. First we perform some algebraic calculations to simplify the integral expression in (28)

$$I_1 = \int_{-h/2}^{h/2} i\omega\varepsilon_o Z G_I E_x dx'$$

$$= \int_{-h/2}^{h/2} i\omega\varepsilon_o Z \left\{ \left[(1/ik_o h) + \sum_{n=1}^{\infty} (2/i\gamma_n h)\cos(2n\pi x/h)\cos(2n\pi x'/h) \right] \right.$$

$$\left. \sum_{m=0}^{\infty} C_n \cos(2m\pi x'/h) \right\} dx'$$

or

$$I_1 = (Z/Z_o)C_o + \sum_{m=1}^{\infty} (Z/Z_n)\cos(2m\pi x/h) C_m \tag{33}$$

and

$$I_2 = i\omega\varepsilon_o Z \int_{-h/2}^{h/2} G_{II} \sum_{m=0}^{\infty} C_m \cos(2m\pi x'/h) dx'$$

$$= (k_o/2)(Z/Z_o) \int_{-h/2}^{h/2} H_o^{(1)}(k_o|x - x'|) \sum_{m=0}^{\infty} C_m \cos(2m\pi x'/h) dx' \tag{34}$$

Equation (28) can now be rewritten as

$$\sum_{m=0}^{\infty} C_m \cos(2m\pi x/h) = 2(Z/Z_o) - \sum_{m=0}^{\infty} (Z/Z_m)\cos(2m\pi x/h)C_m$$

$$\tag{35}$$

$$- (k_o/2)(Z/Z_o) \int_{-h/2}^{h/2} H_o^{(1)}(k_o|x - x'|) \sum_{m=0}^{\infty} C_m \cos(2m\pi x'/h) dx'$$

The second step towards casting (28) into a system of algebraic equations involves the application of the orthogonality properties of the cosine functions (already used in the evaluation of I_1) on (35) to obtain

$$(1 + A_{oo} + Z/Z_o)C_o + \sum_{\ell \neq 0}^{\infty} A_{o\ell}C_\ell = 2(Z/Z_o)$$

<div align="right">(36)</div>

$$[\tfrac{1}{2} + A_{mm} + p_m(Z/2Z_o)]C_m + \sum_{\ell \neq m}^{\infty} A_{m\ell}C_\ell = 0 \qquad m \neq 0$$

where $p_m = k_o/\gamma_m$ and

$$A_{m\ell} = A_{\ell m} = (1/8)(k_o h)(Z/Z_o)\int_{-1}^{+1}\int_{-1}^{+1} H_o^{(1)}[(k_o h/2)|u - u'|]\cos(m\pi u)\cos(\ell\pi u')dudu'$$

<div align="right">(37a)</div>

In appendix III we show that a simple transformation can simplify (37a) and the results are

$$A_{m\ell} = (1/8\pi)(k_o h)(Z/Z_o)\int_0^2 dy H_o^{(1)}(k_o hy/2)\frac{(-1)^{\ell+m+1}}{\ell+m}(\sin \ell\pi y + \sin m\pi y)$$
$$+ \frac{(-1)^{\ell-m+1}}{\ell-m}(\sin \ell\pi y - \sin m\pi y) \qquad \ell \neq m$$

<div align="right">(37b)</div>

$$A_{mm} = -(1/8)(k_o h)(Z/Z_o)\int_0^2 dy H_o^{(1)}(k_o hy/2)[\frac{1}{\pi\ell}\sin \ell\pi y + (y - 2)\cos \ell\pi y] \quad m \neq 0$$

$$A_{oo} = (1/4)(k_o h)(Z/Z_o)\int_0^2 dy(2 - y)H_o^{(1)}(k_o hy/2)$$

For numerical integration the limit $y = 0$ causes difficulties because $H_o^{(1)}$ is singular, therefore the following decomposition is required

$$\int_0^2 dy H_o^{(1)}(\beta y)f(y) = \int_0^2 dy\{H_o^{(1)}(\beta y)f(y) - f(0)[1 + (2i/\pi)[\ln(\beta y/2) + \gamma]]\}$$
$$+ f(0)[2 + 4i\gamma/\pi - 4i/\pi + (4i/\pi)\ln \beta]$$

The above result is based on the limiting form of $H_o^{(1)}$ for small argument

$$H_o^{(1)}(z) \to 1 + (2i/\pi)[\ln(z/2) + \gamma], \qquad z \to 0$$

where $\gamma = .57721566490153$ (Euler's constant). We introduce, as it was done

<div align="center">10</div>

in [2], the parameter β defined by

$$\beta = \frac{cL}{hZ_o} \tag{38}$$

so that

$$Z/Z_o = 1 - i(k_o h)\beta \qquad (R = Z_o) \tag{39}$$

Thus β can be viewed as a normalized inductance and a parametric study on β will determine the optimum L.

Before we solve (36) for a given finite $k_o h$, we examine the two extreme cases of zero and infinite frequencies first. When $k_o h \to 0$ it is easy to show that $A_{m\ell} = 0$ for all m and ℓ. The system of equations (36) is then reduced to

$$C_o = 1 \quad (\Gamma=0), \qquad C_m = 0 \quad m \neq 0$$

Therefore, the choice $R = Z_o$ is indeed a perfect match in the zero frequency limit, i.e., there is no reflection.

Next we consider the case $k_o h \to \infty$. In appendix IV we show that

$$\int_0^2 H_0^{(1)}(k_o h y/2) f(y) dy = f(0)(2/k_o h) + O[(k_o h)^{-3/2}]$$

and if $\beta \neq 0$ equations (37b) yield

$$A_{m\ell} = O[(k_o h)^{\frac{1}{2}}], \qquad m \neq \ell$$

$$A_{mm} = (Z/2Z_o) + [(k_o h)^{\frac{1}{2}}], \quad m \neq 0 \tag{40}$$

$$A_{oo} = Z/Z_o + O[(k_o h)^{\frac{1}{2}}]$$

Substituting equations (40) into (36) we can easily show that as $k_o h \to \infty$, $C_o = 1$ $(\Gamma=0)$ and $C_m = 0$ for $m \neq 0$. The zero inductance case is interesting. For $\beta = 0$ equations (37b) assume the form

11

$$A_{m\ell} = O[(k_o h)^{-\frac{1}{2}}], \qquad m \neq \ell$$

$$A_{mm} = \frac{1}{2} + O[(k_o h)^{-\frac{1}{2}}], \quad m \neq 0$$

$$A_{oo} = 1 + O[(k_o h)^{-\frac{1}{2}}]$$

If we substitute these expressions into (36) we obtain, in the limit $k_o h \to \infty$, $C_o = 2/3$ ($\Gamma = -1/3$) and $C_m = 0$ for $m \neq 0$. This result is not surprising. In the limit of infinite frequency the interaction is local and the situation corresponds to a TEM wave incident upon a infinite (in the xy plane) resistance sheet with $R = Z_o$. The reflection coefficient is given by

$$\Gamma = \frac{Z_L - Z_o}{Z_L + Z_o}$$

where Z_L is the load impedance equal to $Z_o \cdot Z_o / (Z_o + Z_o) = \frac{1}{2} Z_o$. Thus

$$\Gamma = -1/3.$$

After the completion of this work and in an effort to simplify the analysis for the case of a sloped R,L admittance sheet we realized that we can arrive at the systems of equations (36) without using equation (18). The details are given in appendix V.

III. Numerical Results

a. Frequency domain.

In the previous section we determined the C_m's for zero or infinite frequency. For an intermediate frequency we have to solve the system of equations (36) approximately. The solution is based on the assumption that for a given frequency there is an integer N such that all C_M's with M > N are negligibly small compared to the incident field (the choice of M depends on the desired accuracy) and can be set equal to zero. The truncated system of equations can then be solved numerically to determine the C_m's. This must be done for each frequency. Since we also want to calculate the reflections in the time domain we should choose a maximum frequency to use in the Fourier inversion. To do that we should take two factors into account. First, as we showed, in the previous section, in the high frequency limit there is no reflection (if $\beta \neq 0$). Second, our results in the frequency domain correspond to a monochromatic TEM wave or the Fourier transform of a δ-function TEM pulse. In this note we are interested in minimizing the reflections of a TEM step-function pulse and the Fourier transform of u(t) is i/ω. For this case all the reflection coefficients should be multiplied by a term proportional to $1/k_o h$. Therefore, we can select an upper frequency beyond which we can set all the C_m's and Γ equal to zero. How about the case $\beta = 0$? We found that as $k_o h \to \infty$ the C_m's go to zero but $\Gamma \to -1/3$. For the step-function pulse the corresponding Γ in the high frequency limit would be of the order $1/k_o h$ and consequently it would behave like the Fourier transform of a step-function pulse and the initial value of $\Gamma(t)$ should be equal to $-1/3$. (For $\beta \neq 0$, $\Gamma(0+) = 0$.) Thus irrespective of the value of β we will set all the C_m's and Γ equal to zero when the frequency is larger than a maximum one and we will correct the initial value of Γ for the case $\beta = 0$.

Only Γ and the C_m's for the first four TM modes were calculated to any desired accuracy. To obtain this accuracy, the matrix (N×N) that was inverted was progressively larger than 5×5 with increasing frequency. The higher modes (m > 4) have negligibly small amplitudes in the propagating region ($k_o h > 2m\pi$) and even the first four dominant modes decay rapidly with distance in the time domain (see next subsection). The maximum normalized frequency $(k_o h)max$ was chosen equal to fifty. This number is high enough to secure that the reflection coefficients are negligibly small for larger frequencies. In addition $k_o h = 50$ is sufficiently larger than the

resonant (cutoff) frequencies of the first four TM modes. This is important because the reflection coefficients for the field components H_y and E_z are proportional to $\gamma_n^{-1} = k_o^{-1}[1 - (2n\pi/k_o h)]^{-\frac{1}{2}}$ and consequently a Fourier inversion integral should include the region around $k_o h = 2n\pi$ to insure sufficient accuracy (see next subsection).

b.   Time domain.

In this note, we are also interested in the reflected modes if the incident TEM wave is a unit step pulse $E_x^{inc} = u(t - z/c)$. The Fourier transform of a unit step $u(t)$ is i/ω, and consequently we can invert equations (2), (3) and (4) to obtain the reflected modes. If we suppress the x-dependence then the mth modes have the representations

$$E_{mx} = (i/2\pi)\int_{-\infty}^{\infty} (1/k)C_m'(k)\exp[ik(z' - \tau) - ikz'p_m^{-1}]dk, \qquad m \geq 0 \quad (41)$$

$$H_{my} = (-i/2\pi Z_o)\int_{-\infty}^{\infty} C_m'(k)[k^2 - (2m\pi)^2]^{-\frac{1}{2}}\exp[ik(z' - \tau) - ikz'p_m^{-1}]dk, \qquad m \geq 0 \quad (42)$$

$$E_{mz} = (1/2\pi)\int_{-\infty}^{\infty} (2m\pi/k)C_m'(k)[k^2 - (2m\pi)^2]^{-\frac{1}{2}}\exp[ik(z' - \tau) - ikz'p_m^{-1}]dk, m \geq 1 \quad (43)$$

where $p_m^{-1} = \gamma_m/k_o$, $k_o h = k$, $z' = z/h$, $C_m' = C_m$ for $m \neq 0$ and $C_o' = C_o - 1 = \Gamma$. The time variable τ is equal to ct/h and for any cross section $z = z_o$, $\tau = 0$ corresponds to the time when the reflected pulse first hits the plane $z = z_o$. This has been accomplished by multiplying equations (2), (3) and (4) by the correction phase factor $\exp(ikz')$. Thus for $m = 0$ (TEM) the z' dependence disappears, i.e., the amplitude of the TEM reflected pulse suffers no spatial decay as expected. The range of the Fourier integration in equations (41), (42) and (43) involves negative frequencies whereas the system of equation (36) has been solved for positive frequencies only. This does not cause any difficulty because the field components in the time domain are real and the following property exists

$$f(t) = (1/2\pi)\int_{-\infty}^{\infty} F(k)e^{-ik\tau}\,dk$$

$$= (1/2\pi)\int_{0}^{\infty} [F(k)e^{-ik\tau} + F^*(k)e^{ik\tau}]dk \qquad (44)$$

14

An examination of the integrands reveals that they are singular at $k = 0$ and $k = 2m\pi$. The $k = 0$ singularity causes no problem because $C'_m/k \to 0$ as $k \to 0$. The $k = 2m\pi$ singularity is integrable and must be subtracted out to insure accurate numerical integration. This can be done by using the relationship

$$\int_0^\infty \frac{e^{-ik\tau}}{\sqrt{k^2-a^2}} = -i\pi J_0(\tau a) - (\pi/2)Y_0(\tau a) - \int_0^a \frac{\sin k\tau - \sin \tau a}{\sqrt{a^2-k^2}}\,dk - (\pi/2)\sin(\tau a) \quad (45)$$

The integral on the right hand side of (45) can be performed numerically because the integrand vanishes at $k = a$. Notice that $Y_0(\tau a)$ is singular at $\tau = 0$, but as long as τ is different from zero it can assume any desirable small value. To use (45) we rewrite (44) as

$$\int_0^\infty [F(k)e^{-ik\tau} + F^*(k)e^{ik\tau}]\,dk = \int_0^\infty \left[\frac{H(k)}{\sqrt{k^2-a^2}}e^{-ik\tau} + \left(\frac{H(k)}{\sqrt{k^2-a^2}}e^{-ik\tau}\right)^*\right]dk$$

$$= \int_0^\infty \left[\frac{H(k)-H(a)}{\sqrt{k^2-a^2}}e^{-ik\tau} + \left(\frac{H(k)-H(a)}{\sqrt{k^2-a^2}}e^{-ik\tau}\right)^*\right]dk$$

$$+ H(a)\int_0^\infty \frac{e^{-ik\tau}dk}{\sqrt{k^2-a^2}} + \left(H(a)\int_0^\infty \frac{e^{-ik\tau}dk}{\sqrt{k^2-a^2}}\right)^* \quad (46)$$

Equation (46) has now a suitable form for numerical evaluation.

Let us now examine the higher modes to see why they decay with distance. As we mentioned earlier $p_m^{-1} = \gamma_m/k_0$ and

$$\gamma_m = [k_0^2 - (2m\pi/h)^2]^{\frac{1}{2}} \quad \text{for} \quad k_0 > 2m\pi/h$$

$$\gamma_m = i[(2m\pi/h)^2 - k_0^2]^{\frac{1}{2}} \quad \text{for} \quad k_0 < 2m\pi/h$$

Thus

$$\exp[-ikz'p_m^{-1}] = \exp\left[-k|z'|\sqrt{(2m\pi/k)^2 - 1}\right], \quad k_0 < 2m\pi/h, \quad z' < 0 \quad (47)$$

and as $|z'|$ increases the decay becomes more pronounced. Notice, however, that for $k > 2m\pi/h$ there is no decay, therefore, there will be a part of the reflected

pulse (the high frequency part) that will propagate without decay. If we study the plots of the C_m's versus $k_o h$ (Figs. 6, 7, 8 and 9) we can see that they decrease rapidly with frequency for $k_o h > 2m\pi$. Therefore, the propagating part of the reflected pulse will be small. This is demonstrated in Figures 16 through 27. An examination of these plots shows that the pulse suffers little decay from $z/h = -1$ to $z/h = -2$. The reason is, that at $z/h = -1$ most of the spatial decay has already taken place because the exponent in (47) is large (except for k near $2m\pi$).

IV. Description of the Plots

We present plots in the frequency and time domain. In the frequency domain we assume an incident monochromatic TEM wave $E_x^{inc} = e^{ik_0 z}$ and we plot the absolute values of the C_m's, the expansion coefficients of the aperture electric field given by (29), versus $k_0 h$ for the TEM ($m=0$, $\Gamma = C_0 - 1$) and the first four TM modes with β as a parameter. In the time domain the incident TEM wave is a unit step pulse $E_x^{inc} = u(t - z/c)$ and we present plots of the field components given by (41), (42) and (43) versus ct/h. We should mention again that these equations do not include the x-dependence. The total field components for any mode are given by (41), (42) and (43) multiplied by $\cos(2m\pi x/h)$ for E_{mx} and H_{my}, and $\sin(2m\pi x/h)$ for E_{mz}. A detailed description of the plots is given below.

Figure 5. The absolute value of the TEM reflection coefficient is plotted versus $k_0 h$ with β as a parameter. For an incident monochromatic TEM wave with a frequency below cutoff the choice of L should be made by studying this plot.

Figure 6
to 9. Plots of the absolute values of the transverse electric field component reflection coefficients for the first four TM modes versus $k_0 h$ with β as a parameter. For an incident monochromatic TEM wave with a frequency above cutoff for one or more TM modes a study of Figs. 5 through 9 will allow the determination of the optimum L to minimize the overall reflection.

The rest of the figures are plots in the time domain when the incident wave is a unit step-function TEM pulse $E_x^{inc} = u(t - z/c)$.

Figures 10
and 11. Plots of the negative of the electric field component of the TEM reflected pulse versus ct/h with β as a parameter. Since all the reflected TM modes decay with distance considerably (see figures below) this plot is the only one that was studied to determine the value of $L = \beta h Z_0/c = (1.1 h Z_0)/c$ to minimize the overall TEM

reflection. The reason for plotting the negative of the field
component was a sign mistake in the data which was not detected
until all the time plots were completed.

The subsequent figures are plots of reflected TM field components versus ct/h
with the x-dependence suppressed.

Figures 12

to 15.   Plots of the negative of the transverse electric field component for
               the first four TM modes versus ct/h with β as a parameter at z = 0.
               These plots serve to illustrate the relative dependence of the TM
               modes on β in the time domain.

The decay of the reflected TM modes with distance is demonstrated in figures
16 through 27 by plotting the field components at three planes, i.e.,
z/h= 0, -1, -2 for β = 1.1. When the field amplitude was diminutive only
the z/h= 0 and z/h = -1 cases were considered.

Figures 16

to 19. $-E_{mx}$ versus ct/h at z/h= 0, z/h = -1, z/h = -2 for β = 1.1 with
               m = 1, 2, 3, 4.

Figures 20

to 23. $-E_{mz}$ versus ct/h at z/h= 0, z/h = -1, z/h = -2 for β = 1.1 with
               m = 1, 2, 3, 4.

Figures 24

to 27. $-H_{my}$ versus ct/h at z/h= 0, z/h = -1, z/h = -2 for β = 1.1 with
               m = 1, 2, 3, 4.

Appendix I

We want to show that if E_x given by (29) is substituted into (23) the resulting expression for H_{Iy} is equation (2). We rewrite (23) as

$$H_{Iy} = (1/Z_o(e^{ik_oz} + e^{-ik_oz}) - \int_{-h/2}^{h/2} i\omega\varepsilon_o \sum_{m=0}^{\infty} C_m \cos(2m\pi x/h)$$

$$\left[(1/ik_oh)e^{-ik_oz} + \sum_{n=1}^{\infty} (2/i\gamma_n h)\cos(2n\pi x/h)\cos(2n\pi x'/h)e^{-i\gamma_n z} \right]dx'$$

Performing the integration we obtain

$$H_{Iy} = (1/Z_o)(e^{ik_oz} + e^{-ik_oz}) - \frac{\omega\varepsilon_o}{kh} C_o he^{-ik_oz}$$

$$- \sum_{n=1}^{\infty} \frac{2\omega\varepsilon_o}{\gamma_n h} C_m(h/2)\cos(2n\pi x/h)e^{-i\gamma_n z}$$

Noting that $C_o = 1 + \Gamma$, $\varepsilon_o c = Z_o^{-1}$, $\omega\varepsilon_o/\gamma_n = Z_n^{-1}$ we can easily see that the above equation is the same as (2).

It is also easy to show that if E_x given by (29), $H_{Iy}(x',0)$ given by (3) and G_I by (30) are substituted in the integral of equation (20) the resulting $H_{Iy}(x,z)$ is identical to equation (3). This indicates the validity of equation (30) for the Green's function G_I.

Appendix II

In this appendix we show that the pair of equations (20) and (21) applied at $z = 0$, together with the boundary condition (27) lead to (28). We start with (20) by evaluating $\partial G_I/\partial z'$. G_I is given by (30) and we want to take the derivative with respect to z' and set $z' = 0$. Eventually we will also set $z = 0$. When $z' = 0$ and z negative, (30) can be written as

$$G_I = (1/2ik_o h)e^{ik_o(z'-z)} + \sum_{n=1}^{\infty} (1/i\gamma_n h)\cos(2n\pi x/h)\cos(2n\pi x'/h)e^{i\gamma_n(z'-z)} \qquad \text{(II-1)}$$

Taking the derivative of (II-1) with respect to z' and setting $z' = 0$ we obtain

$$\partial G_I/\partial z' = (1/2h)e^{-ik_o z} + \sum_{n=1}^{\infty} (1/h)\cos(2n\pi x/h)\cos(2n\pi x'/h)e^{-i\gamma_n z} \qquad \text{(II-2)}$$

Using (II-2), (20) can be written as

$$H_{Iy}(x,z) = (1/Z_o)e^{ik_o z} + \int_{-h/2}^{h/2} \Bigg\{ -i\omega\varepsilon_o E_x G_I$$

$$+ \left[(1/2h)e^{-ik_o z} + \sum_{n=1}^{\infty} (1/h)\cos(2n\pi x/h)\cos(2n\pi x'/h)e^{-i\gamma_n z} \right] H_{Iy} \Bigg\} dx' \qquad \text{(II-3)}$$

Now we let $z \to 0$ in (II-3). Recall that

$$1/2h + \sum_{n=1}^{\infty} (1/h)\cos(2n\pi x/h)\cos(2n\pi x'/h) = (1/2)\delta(x - x') \qquad \text{(II-4)}$$

Substituting (II-4) in (II-3) we obtain

$$H_{Iy}(x,0) = (1/Z_o) + \int_{-h/2}^{h/2} - i\omega\varepsilon_o E_x G_I dx' + (1/2)H_{Iy}(x,0)$$

or

$$H_{Iy}(x,0) = (2/Z_o) + \int_{-h/2}^{h/2} - i\omega\varepsilon_o E_x (2G_I) dx' \qquad \text{(II-5)}$$

Observe now that at $z' = z = 0$

$$2G_I = G'_I$$

and consequently (II-5) coincides with (23) evaluated at $z = 0$ because

$$H_o = (1/Z_o)(e^{ik_o z} + e^{-ik_o z})\bigg|_{z=0} = 2/Z_o$$

The subsequent derivation of (28) is the one given earlier. A last point has to be clarified. Notice that equation (26) should coincide with (II-5). A cursory examination may indicate that this is not true, that is, it seems that the term

$$\int_{-h/2}^{h/2} \frac{\partial G_I}{\partial z'} H_{Iy} dx'$$

would contribute $(1/2)H_{Iy}$ as we showed earlier. If this is the case, (II-5) is different from (26). The resolution of the paradox lies in the observation that the integral in equation (26) is a principal value integral, that is, a small region around $x' = x$ must be excluded. In that case the integral of the δ-function vanishes and the term

$$\int_{-h/2}^{h/2} \frac{\partial G_I}{\partial z'} H_{Iy} dx'$$

contributes zero.

Appendix III

We want to simplify the double integral

$$I = \int_{-1}^{+1} du \int_{-1}^{+1} du' H_o^{(1)} [(\beta h/2)|u - u'|] \cos(m\pi u)\cos(\ell\pi u') \qquad \text{(III-1)}$$

We make the following transformation

$$u = u$$
$$u - u' = y$$

In figure 4 we show how the domain of integration is transformed. The Jacobian is equal to unity. Referring to figure 4 we can rewrite (III-1) as

$$I = \int_{-2}^{o} dy \int_{-1}^{1+y} du \, \cos m\pi u \, \cos[\ell\pi(u - y)] H_o^{(1)} [(\beta h/2)|y|]$$

$$+ \int_{o}^{2} dy \int_{y-1}^{1} du \, \cos m\pi u \, \cos[\ell\pi(u - y)] H_o^{(1)} [(\beta h/2)y] \qquad \text{(III-2)}$$

If we set $u \to - u$, $v \to - v$ in the first integral in (III-2) we can see that it is equal to the second one and I becomes

$$I = 2 \int_{o}^{2} dy H_o^{(1)} [(\beta h/2)y] \int_{y-1}^{1} \cos \ell\pi(u - y)\cos m\pi u du \qquad \text{(III-3)}$$

We can easily perform the u-integration to arrive at the expressions for $A_{\ell m}$ given earlier.

Appendix IV

In this appendix we make an asymptotic evaluation of the coefficients $A_{\ell m}$ as $k_o h \to \infty$. Consider the integral

$$I = \int_0^2 H_0^{(1)}(\beta y) f(y) dy, \qquad \beta = k_o h/2 \qquad (IV-1)$$

An examination of equations (37b) reveals that $f(y)$ can be expanded in a Maclaurin series, i.e.,

$$I = \int_0^2 H_0^{(1)}(\beta y)[f(0) + y f'(0) + \cdots] dy \qquad (IV-2)$$

First we examine

$$I_o = \int_0^2 H_0^{(1)}(\beta y) dy \qquad (IV-3)$$

Using the integral representation

$$H_0^{(1)}(\beta y) = (-2i/\pi) \int_0^\infty e^{i\beta y \cosh t} dt \qquad (IV-4)$$

in (IV-3) and interchanging the order of integrations we obtain

$$I_o = (-2i/\pi) \int_0^\infty dt \int_0^2 e^{i\beta y \cosh t} dy$$

$$= -(2/\pi\beta) \int_0^\infty dt \frac{e^{2i\beta \cosh t}}{\cosh t} + (1/\pi\beta) \int_0^\infty \frac{dt}{\cosh t}$$

$$I_o = -(2/\pi\beta) \int_0^\infty dt \frac{e^{2i\beta \cosh t}}{\cosh t} + 1/\beta \qquad (IV-5)$$

As $\beta \to \infty$ we can use stationary phase to show that

$$\int_0^\infty dt \frac{e^{2i\beta \cosh t}}{\cosh t} = 0(\beta^{-\frac{1}{2}})$$

and (IV-5) gives

23

$$I_o = 1/\beta + O(\beta^{-3/2}) \qquad\qquad (IV\text{-}7)$$

If we evaluate the rest of the terms in (IV-2) we find that the dominant term is of order $\beta^{-3/2}$ and consequently we can rewrite (IV-1) as

$$I = \int_o^2 H_o^{(1)}[(k_o h/2)y]f(y)dy = f(0)(2/k_o h) + O[(k_o h)^{-3/2}].$$

Appendix V

The systems of equations (36) can be alternately derived as follows. We start with boundary condition (27) and substitute H_{IIy} by its integral representation (21).

$$E_x = ZH_{Iy} - Z \int_{-h/2}^{h/2} i\omega\epsilon_o E_x G_{II} dx' \qquad (V-1)$$

From equations (2) and (3) we find that

$$E_x(x,0) = 1 + \Gamma + \sum_{m=1}^{\infty} C_m \cos(2m\pi x/h) \qquad (V-2)$$

$$H_{Iy}(x,0) = (1 - \Gamma)/Z_o - \sum_{m=1}^{\infty} (C_m/Z_m)\cos(2m\pi x/h) \qquad (V-3)$$

The electric field E_x is continuous across the admittance sheet, therefore we can combine the previous equations to obtain

$$\sum_{m=0}^{\infty} C_m \cos(2m\pi x/h) = 2Z/Z_o - Z \sum_{m=0}^{\infty} (C_m/Z_m)\cos(2m\pi x/h)$$

$$- i\omega\epsilon_o Z \int_{-h/2}^{h/2} \sum_{m=0}^{\infty} C_m \cos(2m\pi x'/h)G_{II} dx' \qquad (V-4)$$

Application of orthogonality relations of the cosine functions on (V-4) yields the desired system of equations (36). The above formulation avoids the questions arising from using the Green's function G_I, but it also confirms the validity of representation (30). Naturally, the relationship between the coefficients of the expansion of the aperture electric field to the coefficients of the expansion of the interior aperture magnetic field is contained in equation (18) which was omitted in the above formulation.

25
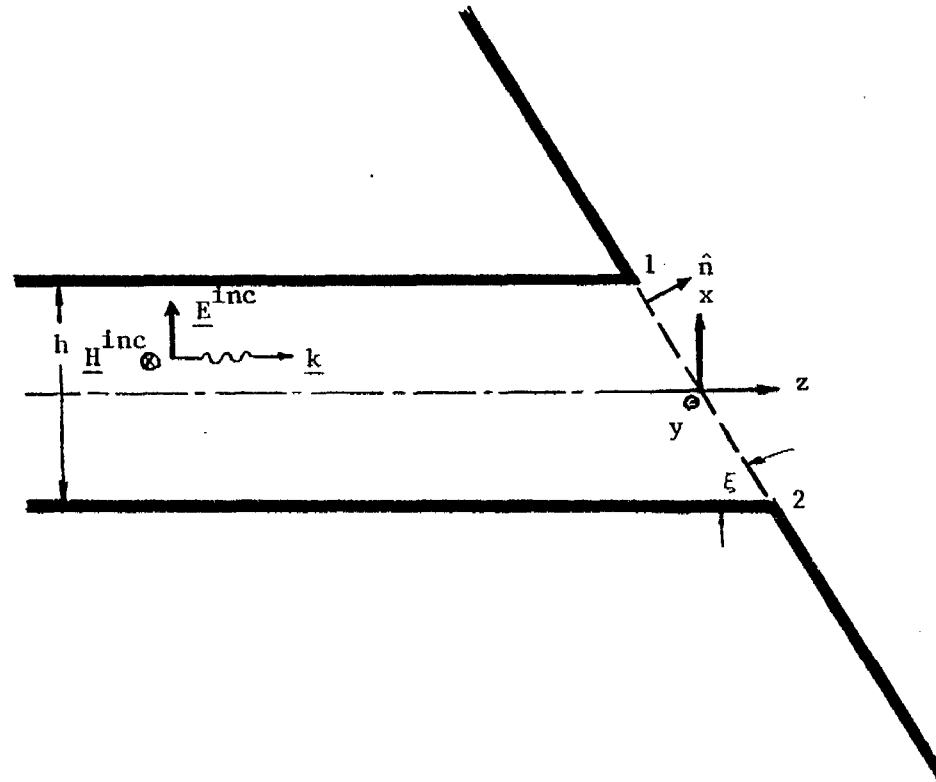
Figure 1. Geometry of the two-dimensional parallel-plate transmission line
terminated by a sloped R,L admittance sheet with coplanar
conducting flanges.

Figure 2. Regions I and II used to derive the integral relationships in the text.
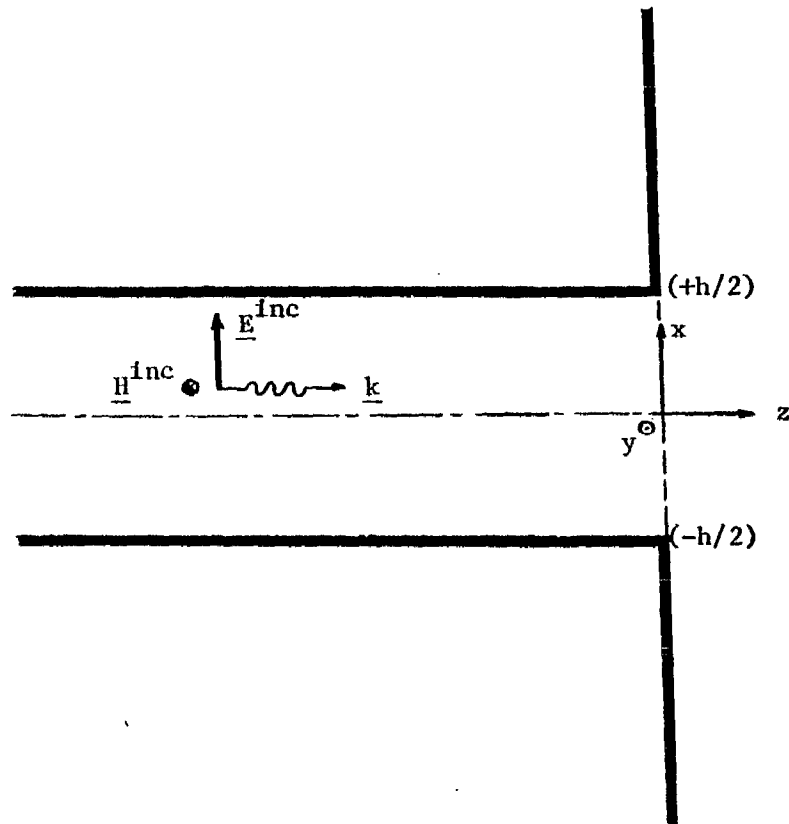
Figure 3. Geometry of the transmission line with a perpendicular
admittance sheet considered in detail in this note.
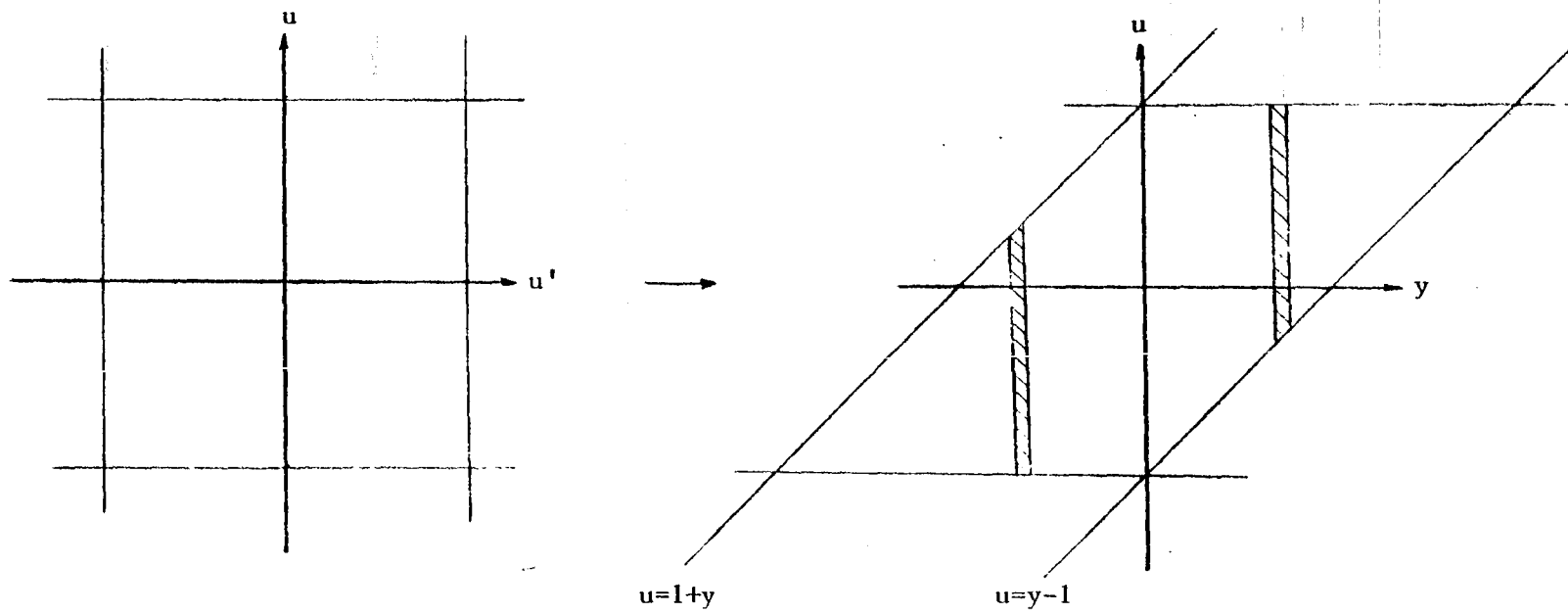
Figure 4. Integration regions resulting from transformation of variables u,u' to u,y.
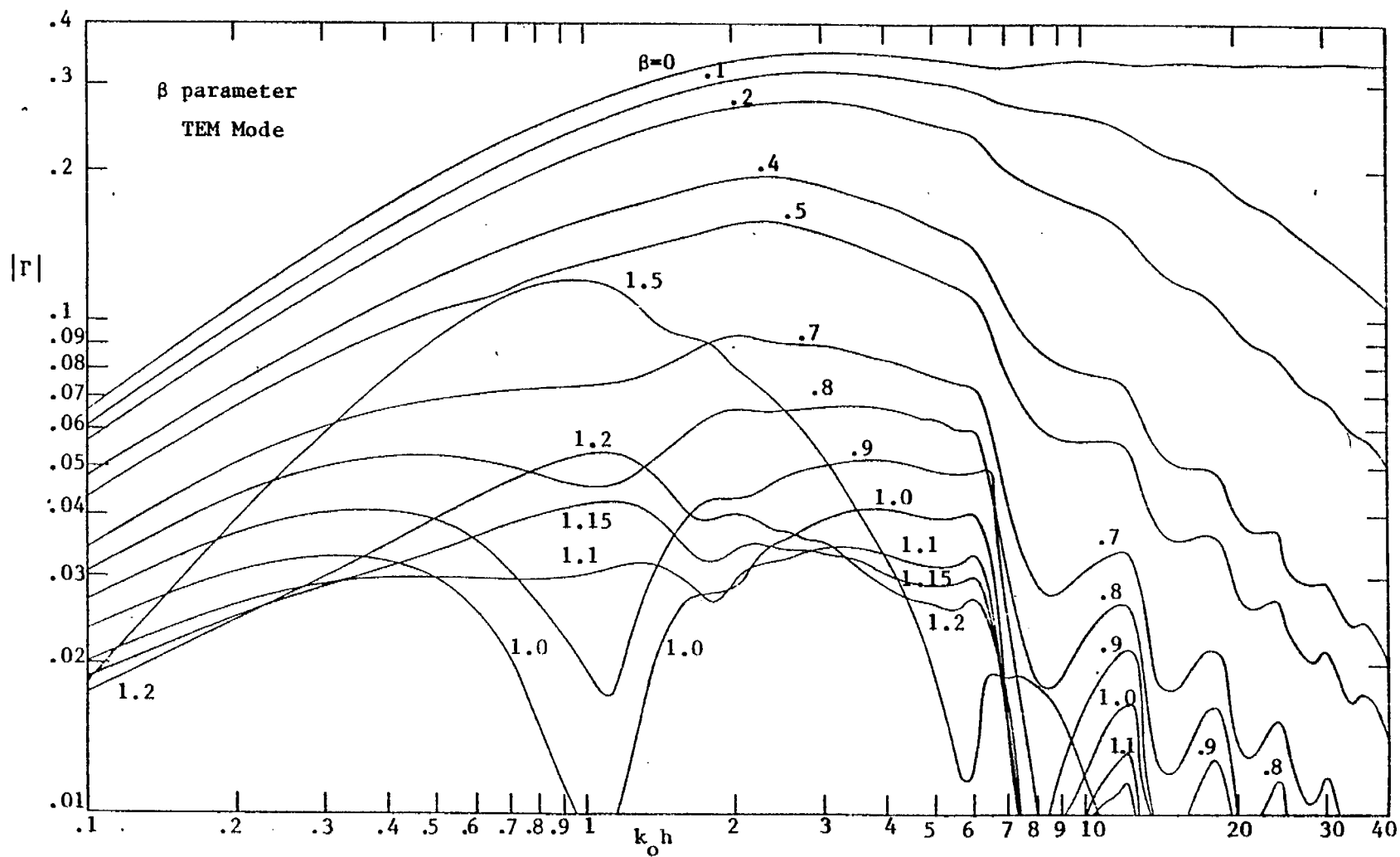
Figure 5
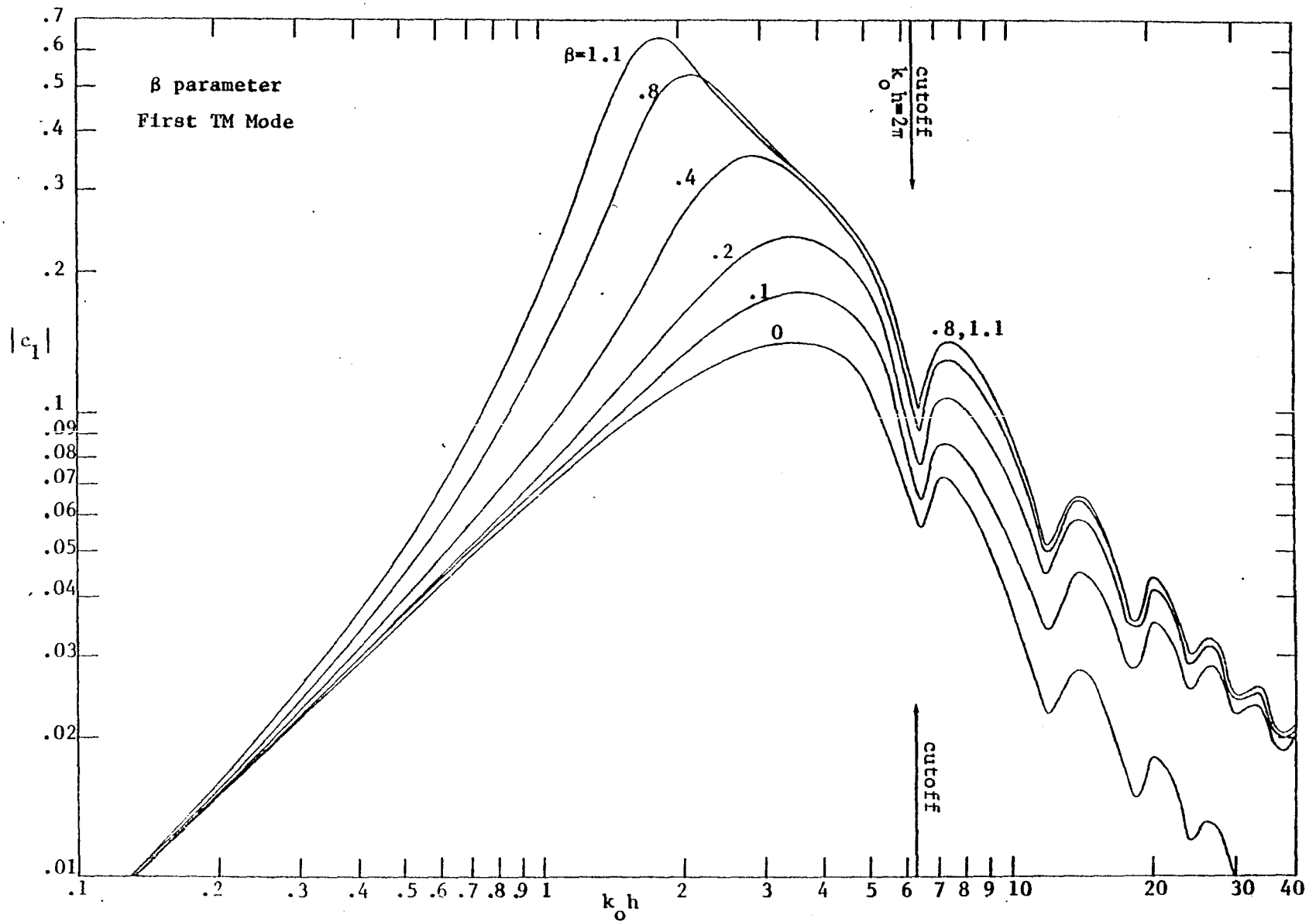
Figure 6
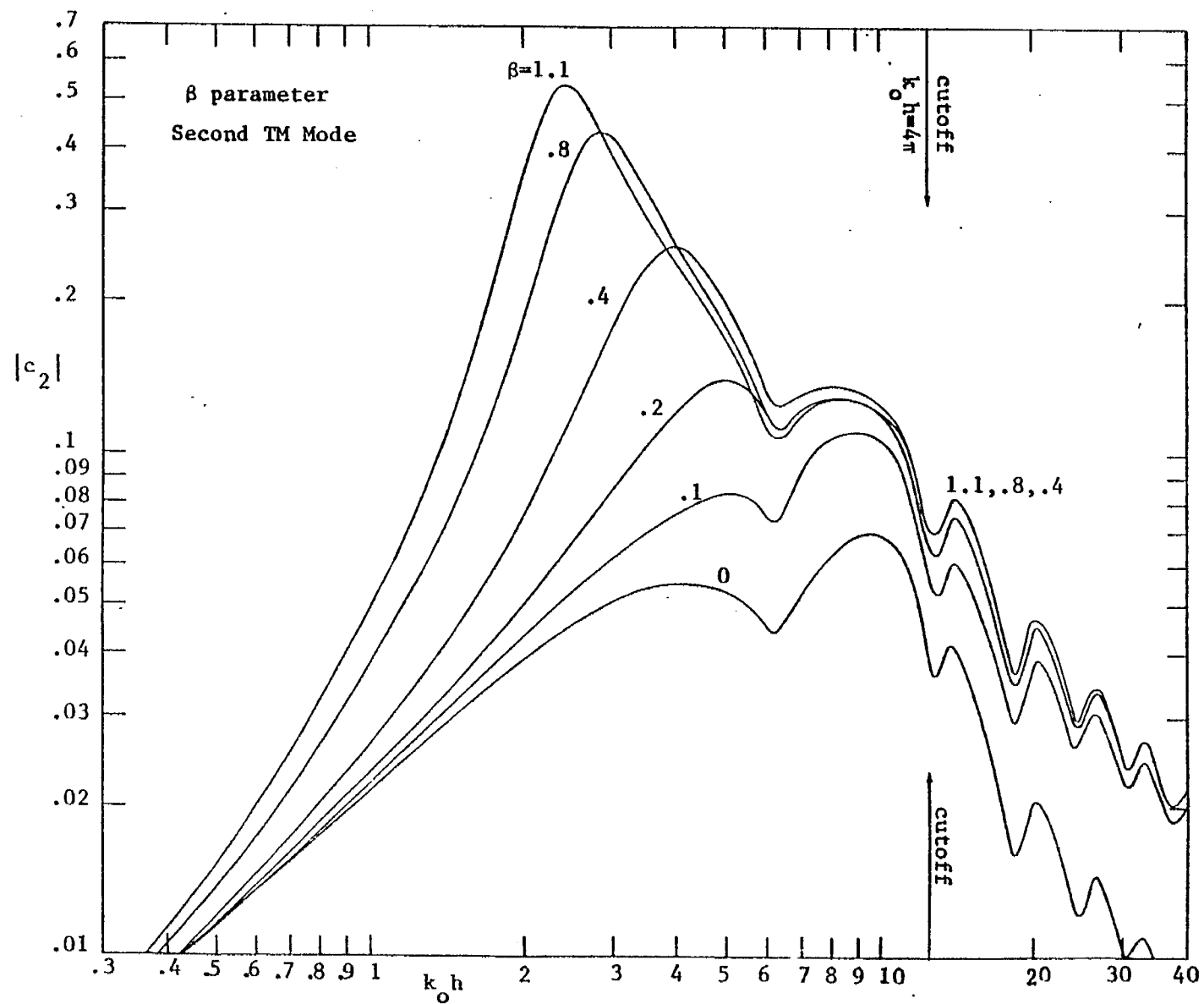
Figure 7

Figure 8

Figure 9

34
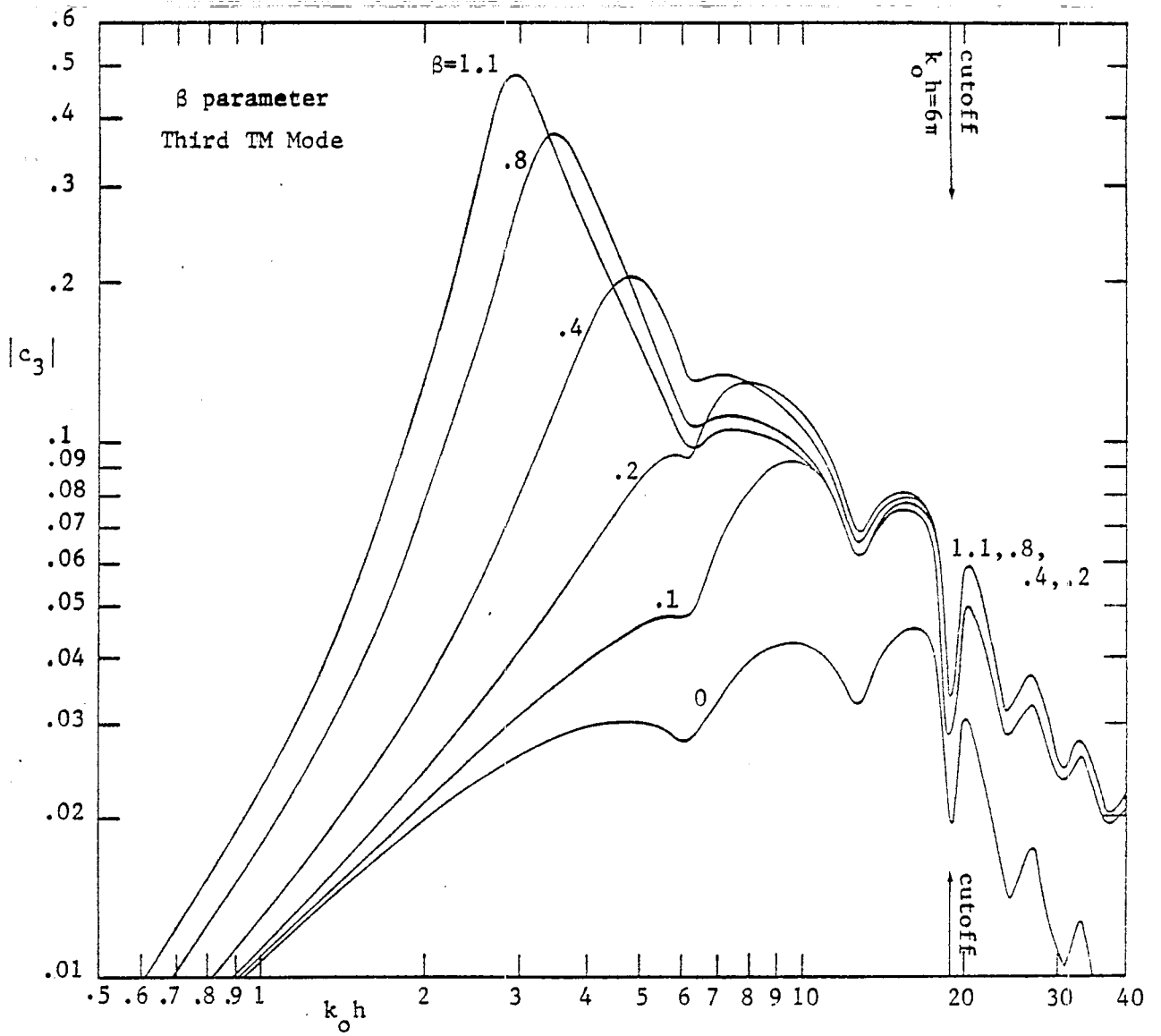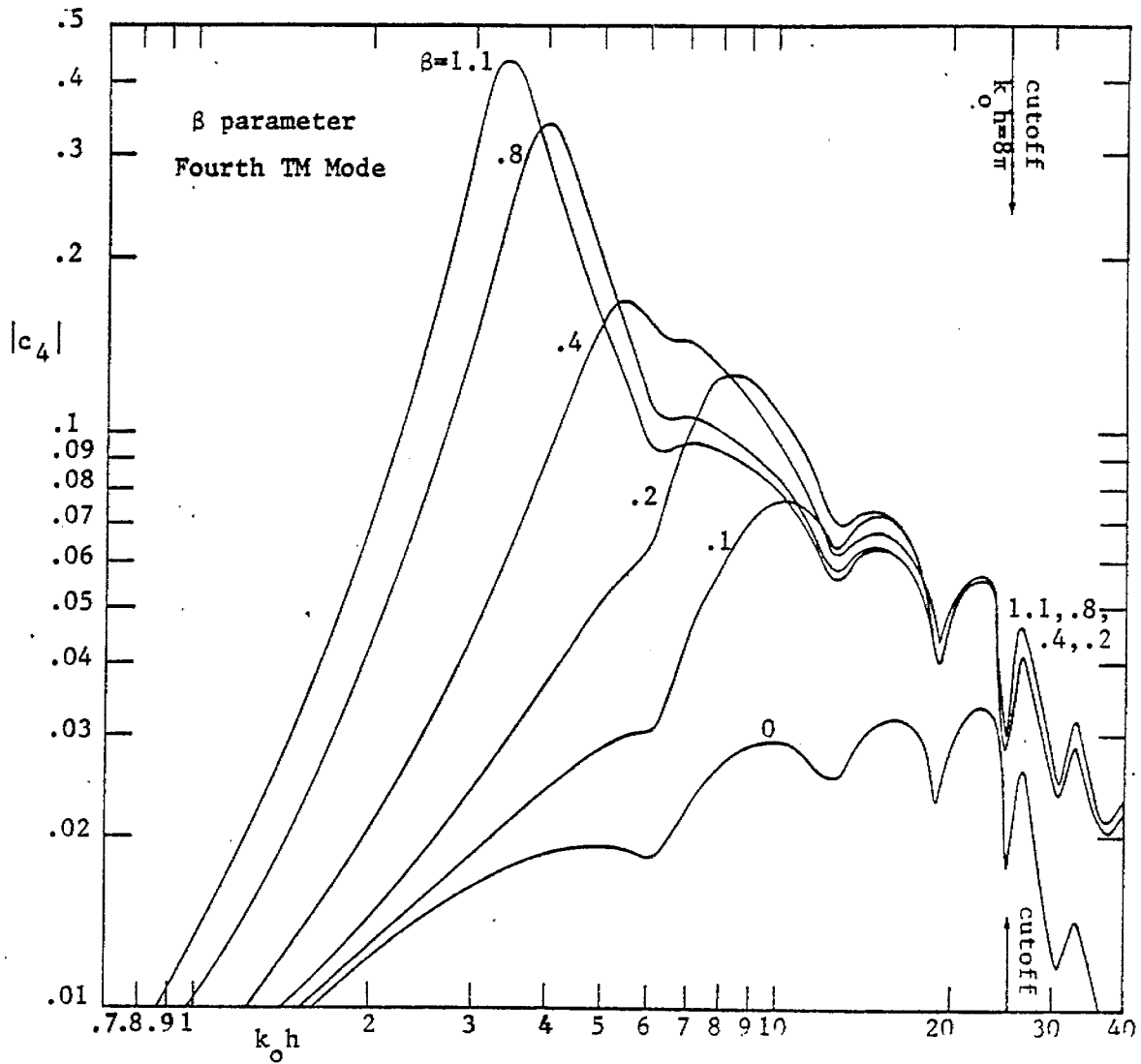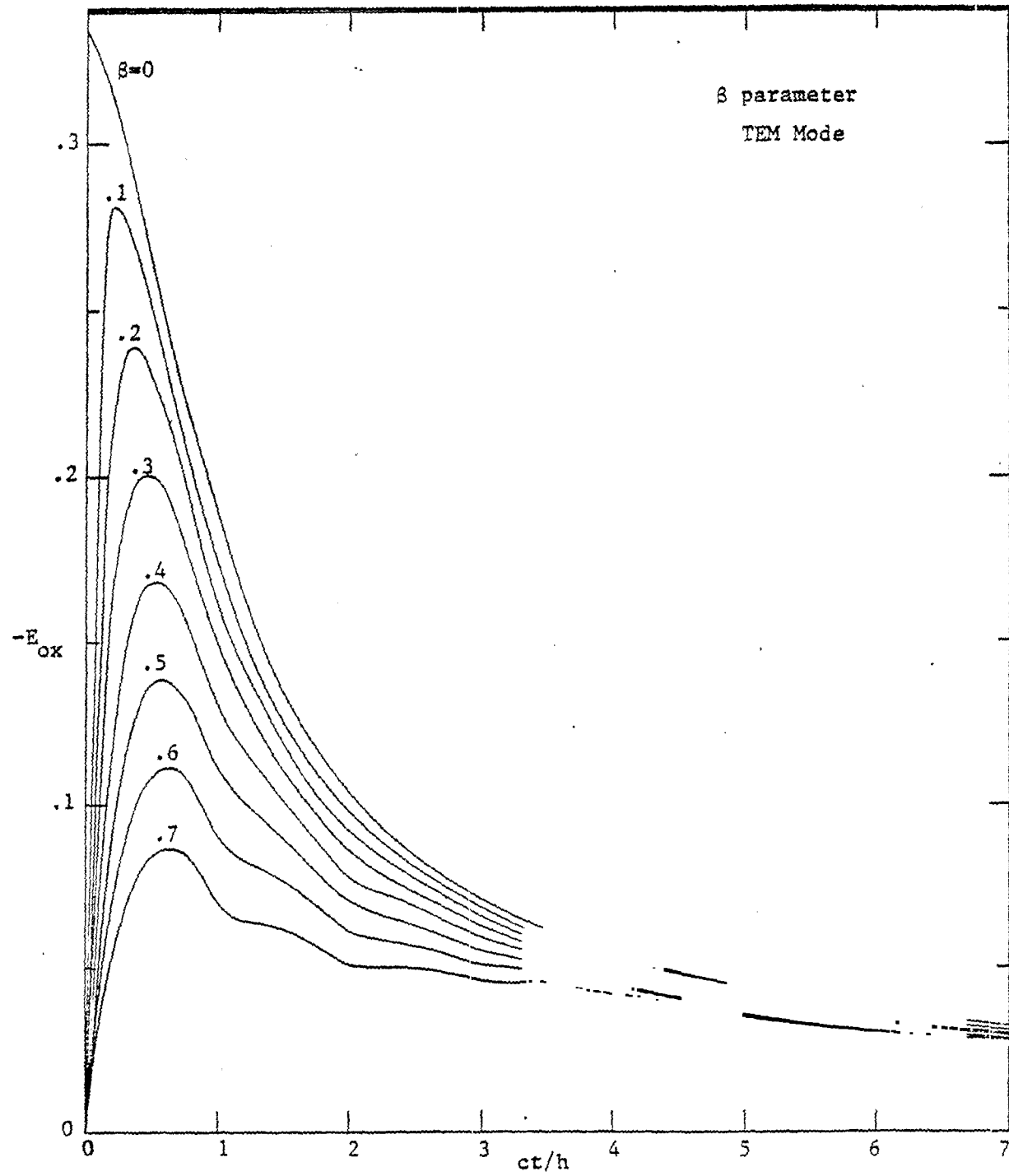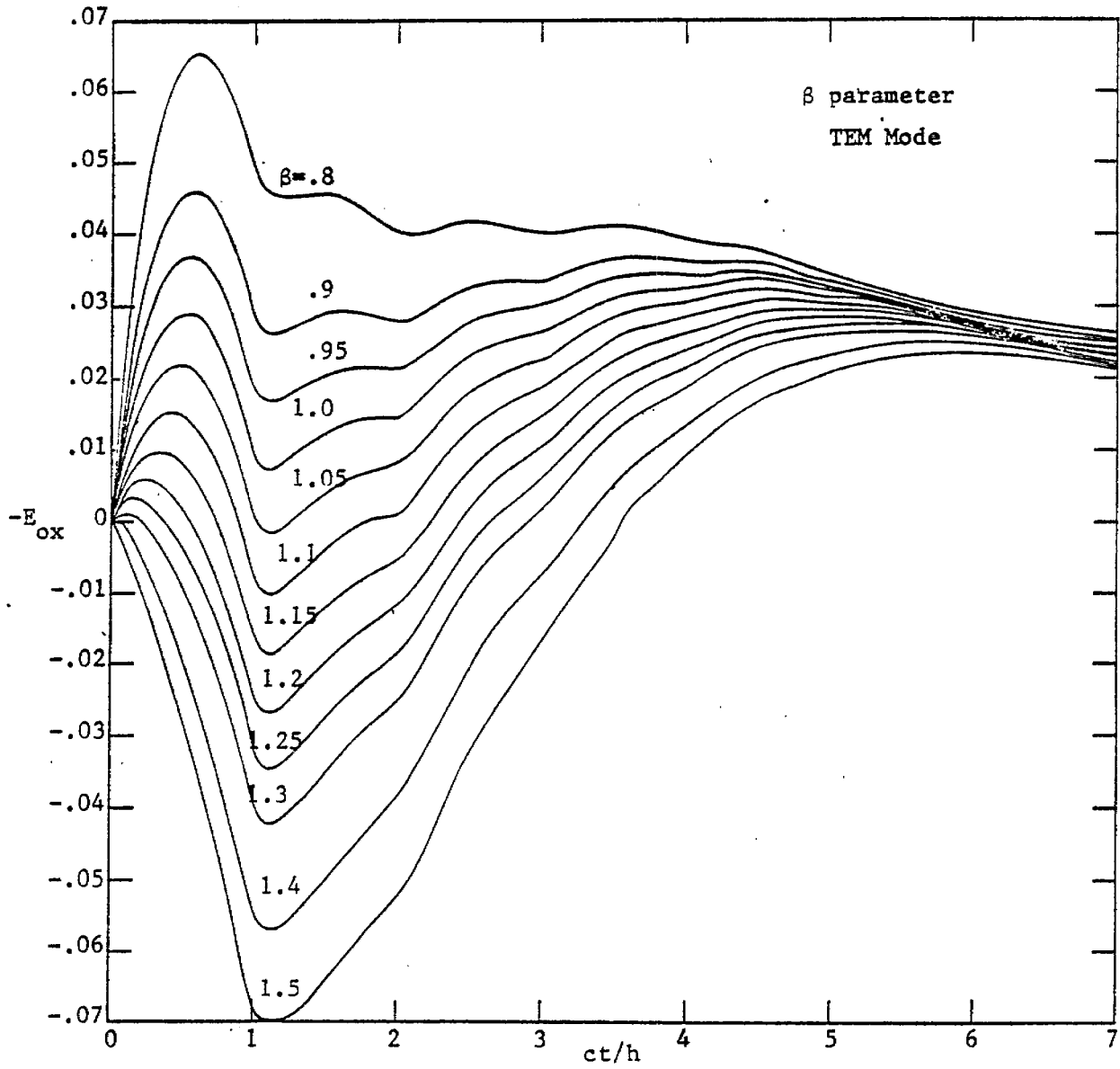
Figure 10

Figure 11
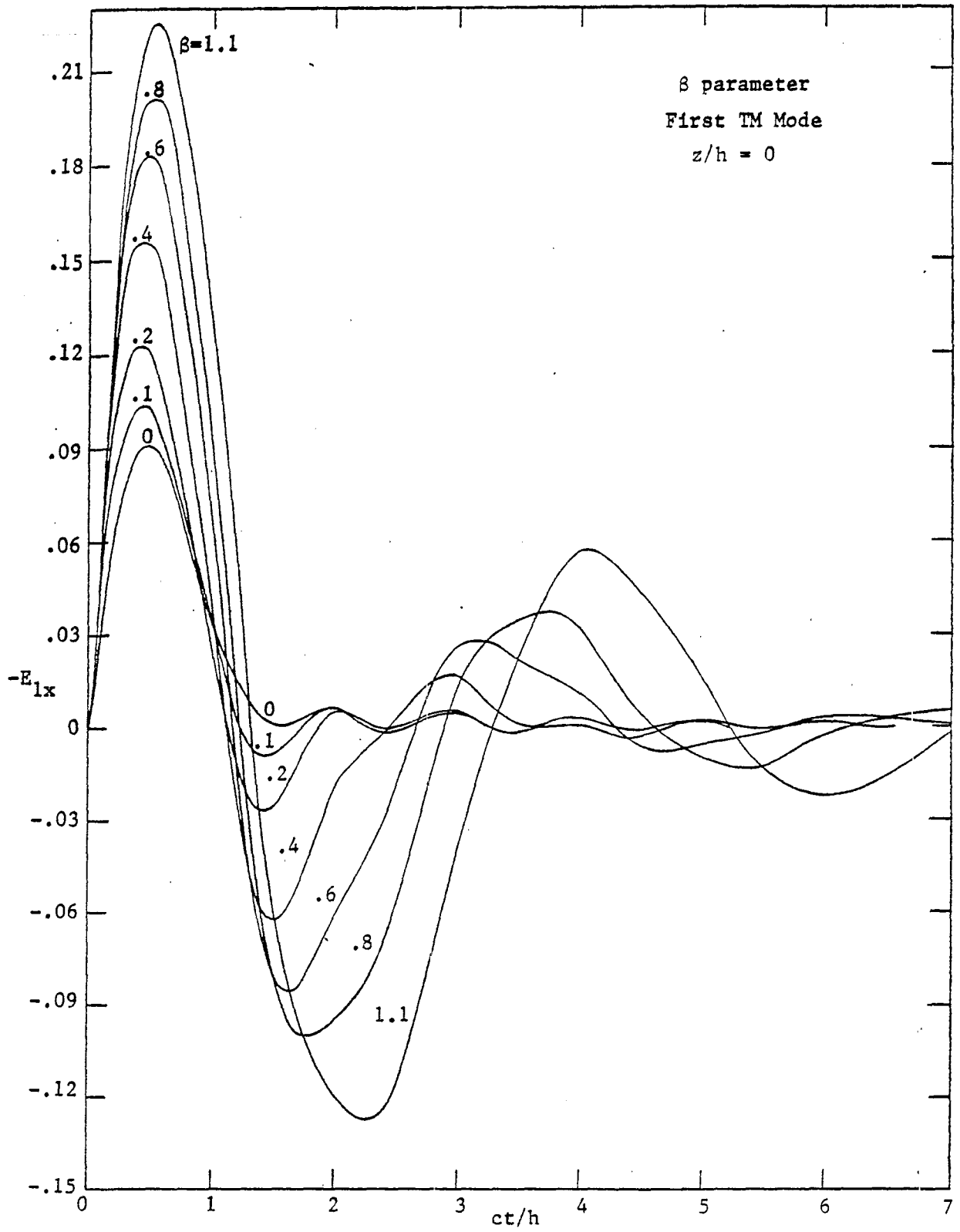
Figure 12
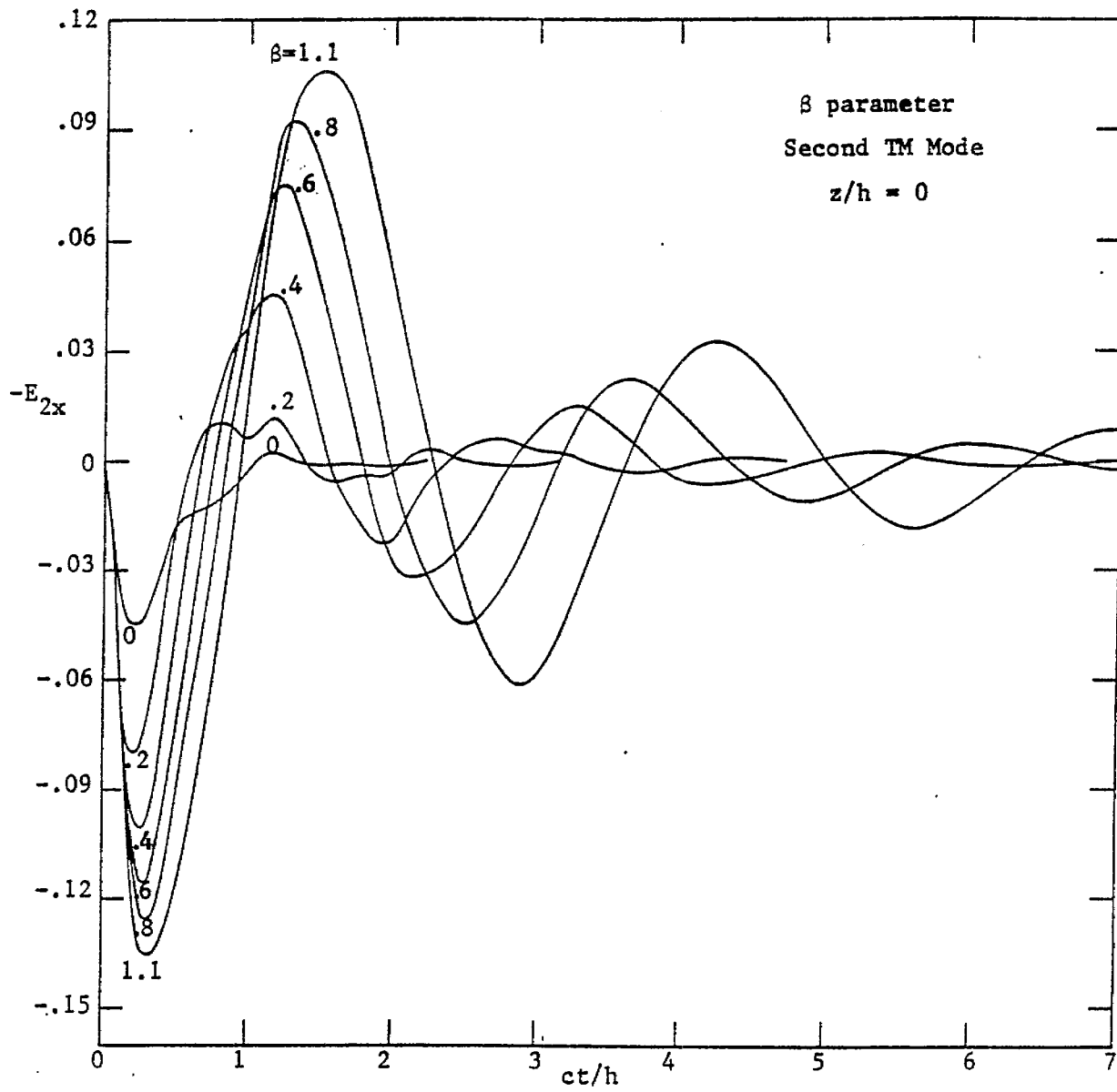
Figure 13
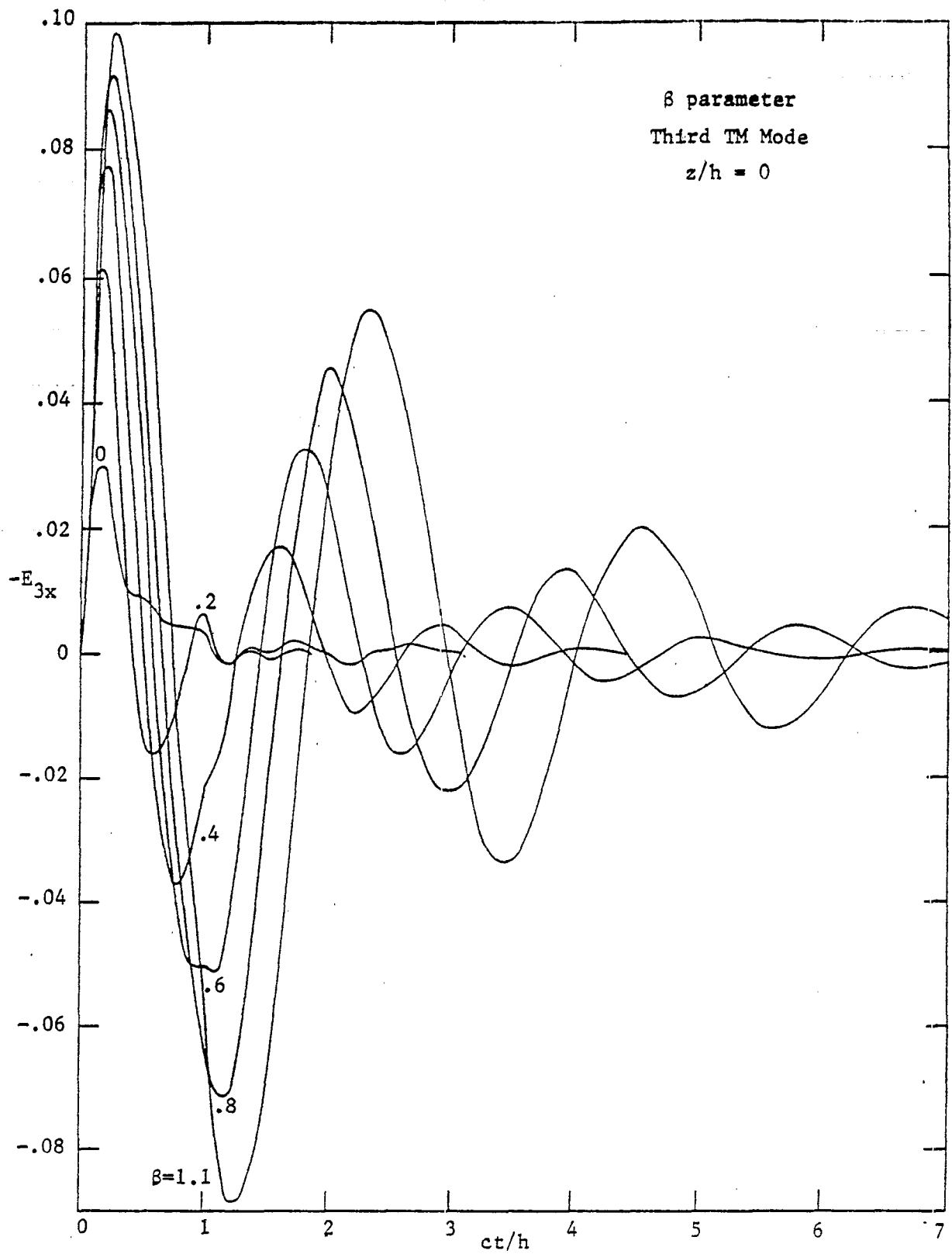
Figure 14
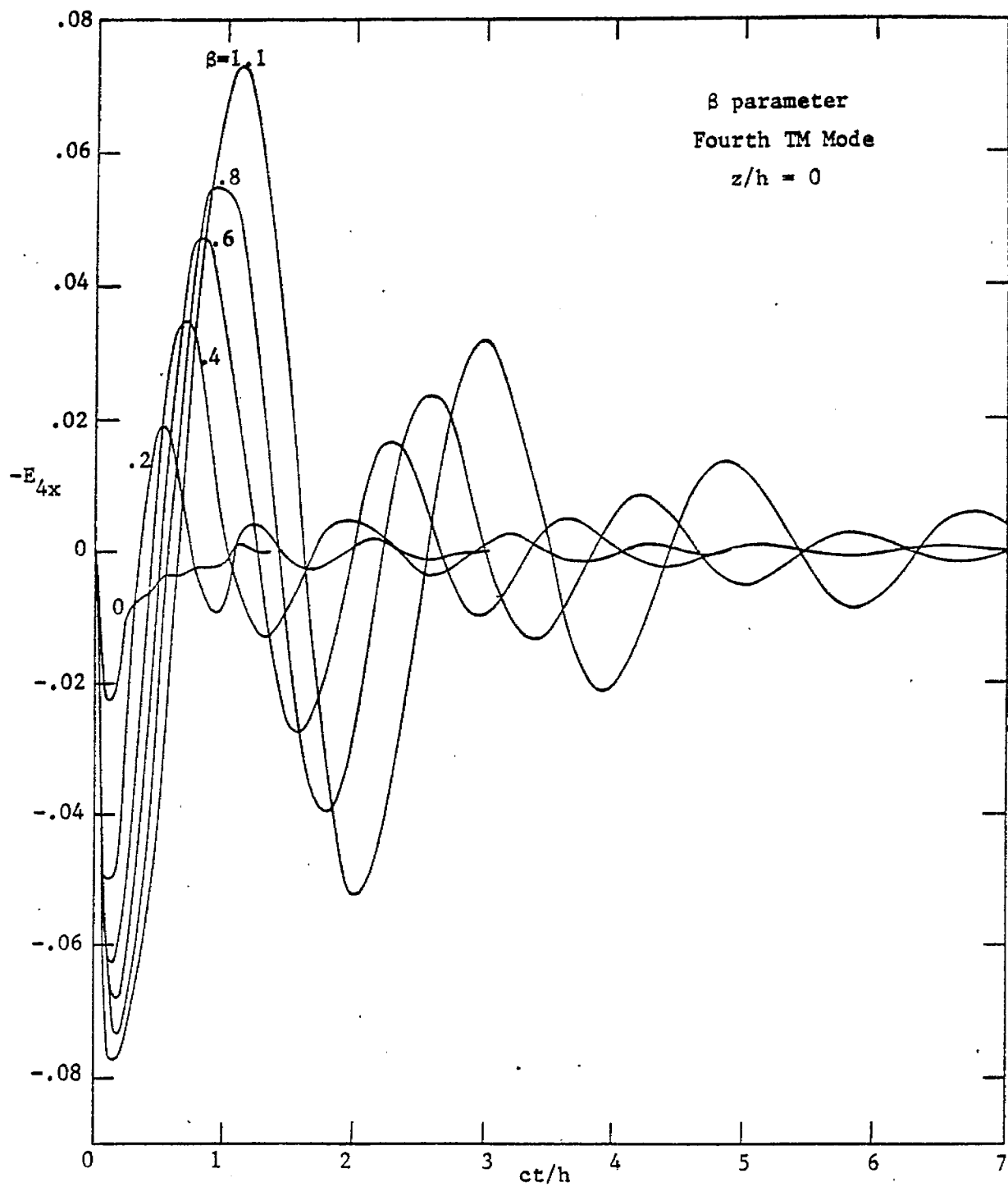
Figure 15

Figure 16

41
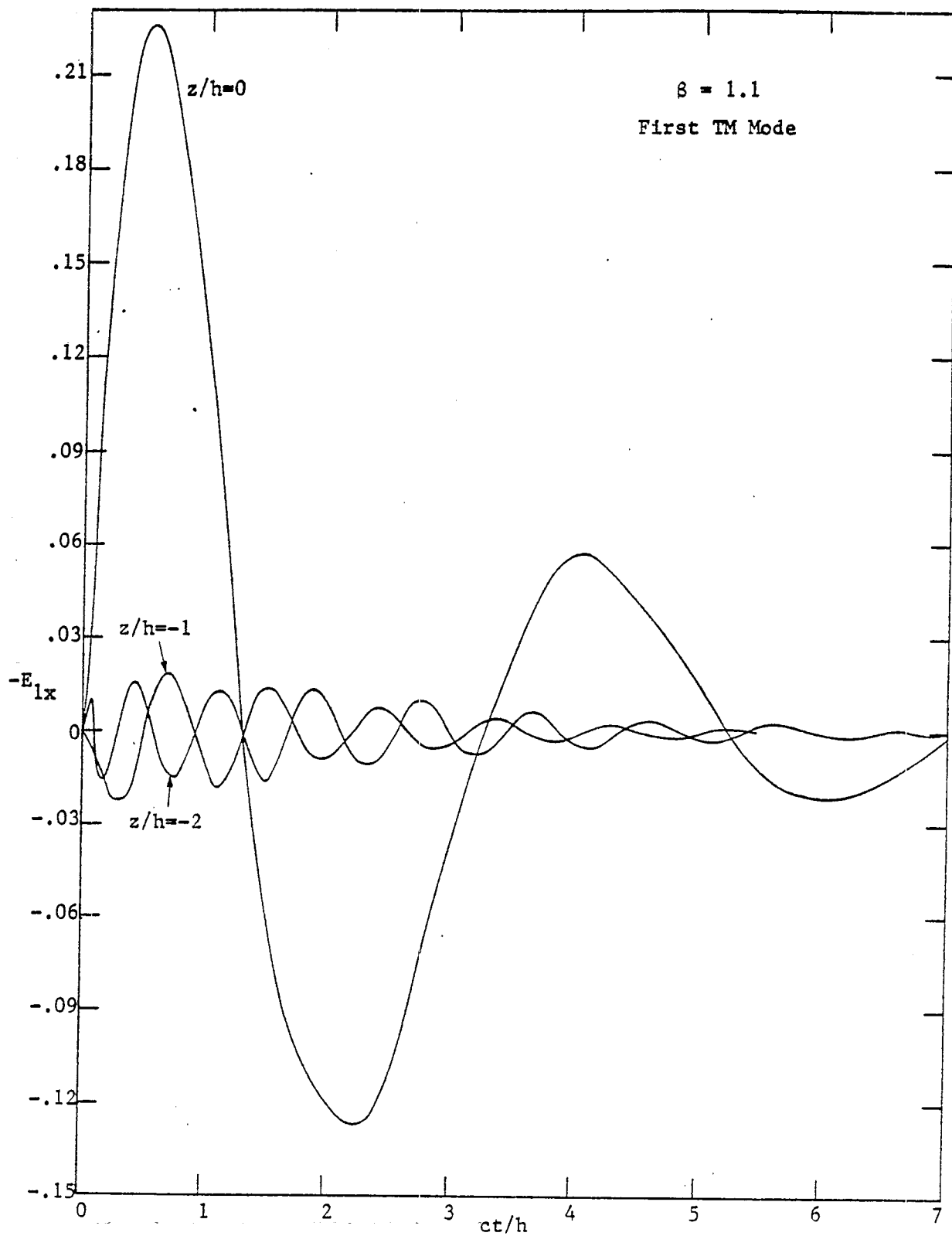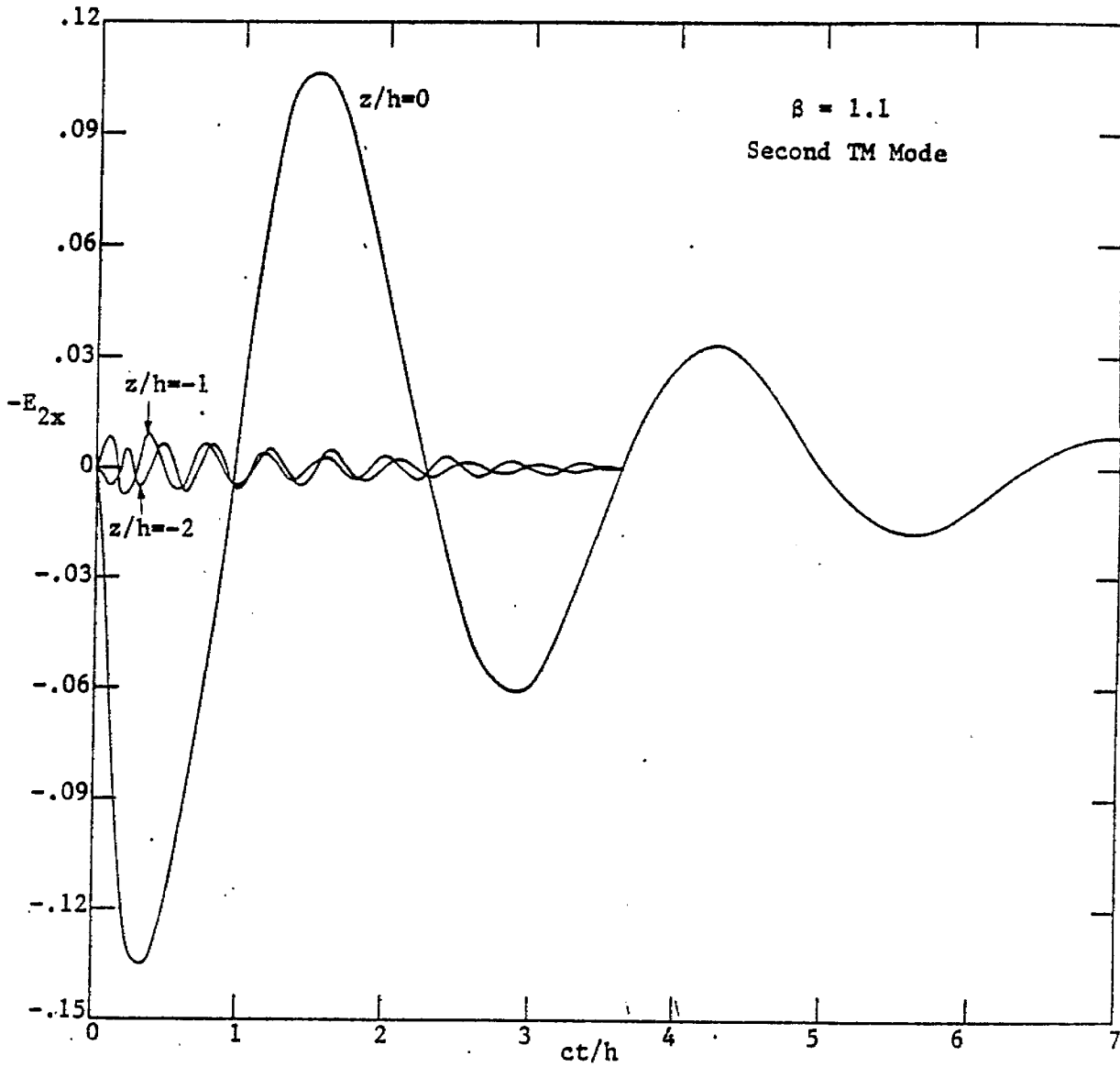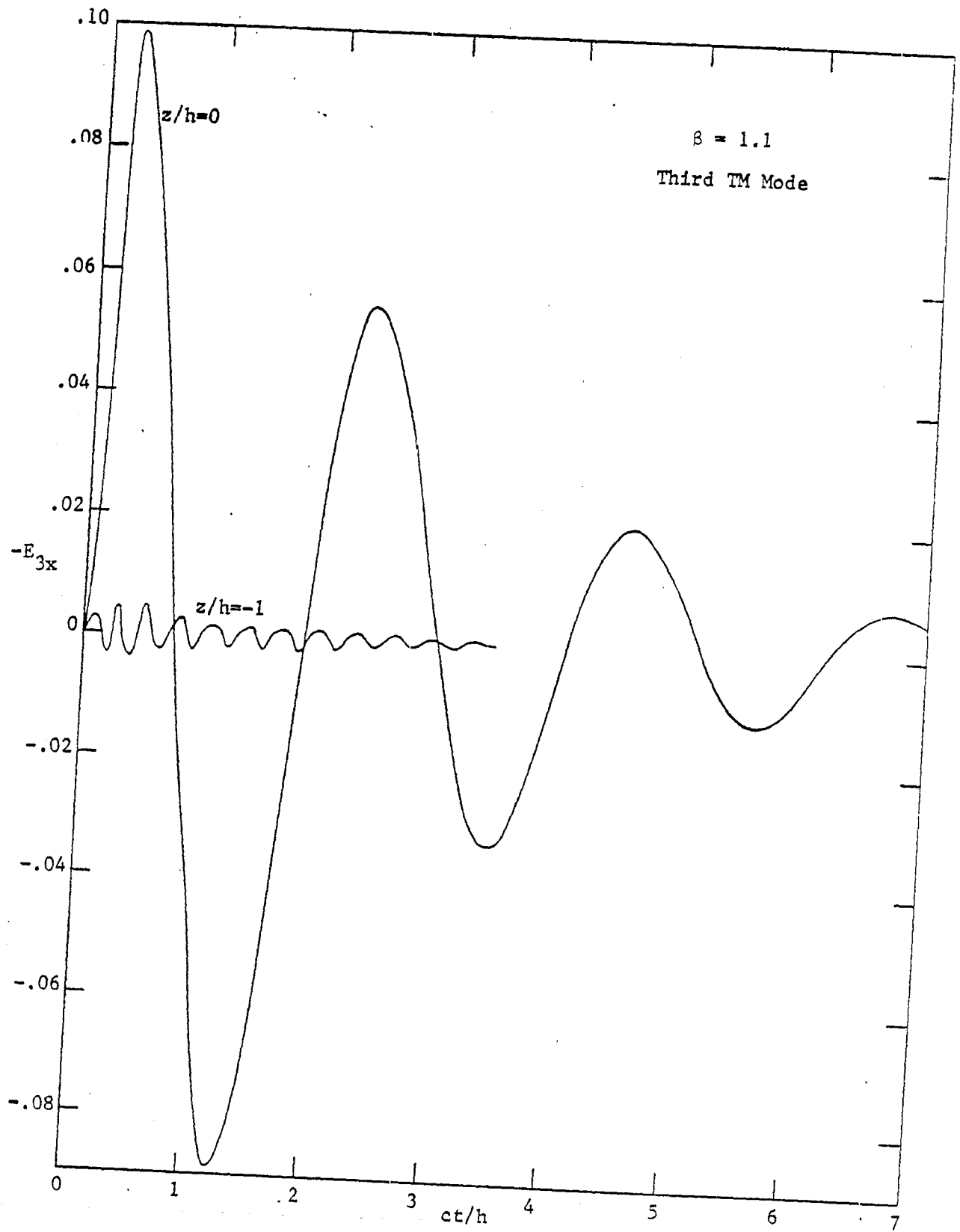
Figure 17

Figure 18

Figure 19

44
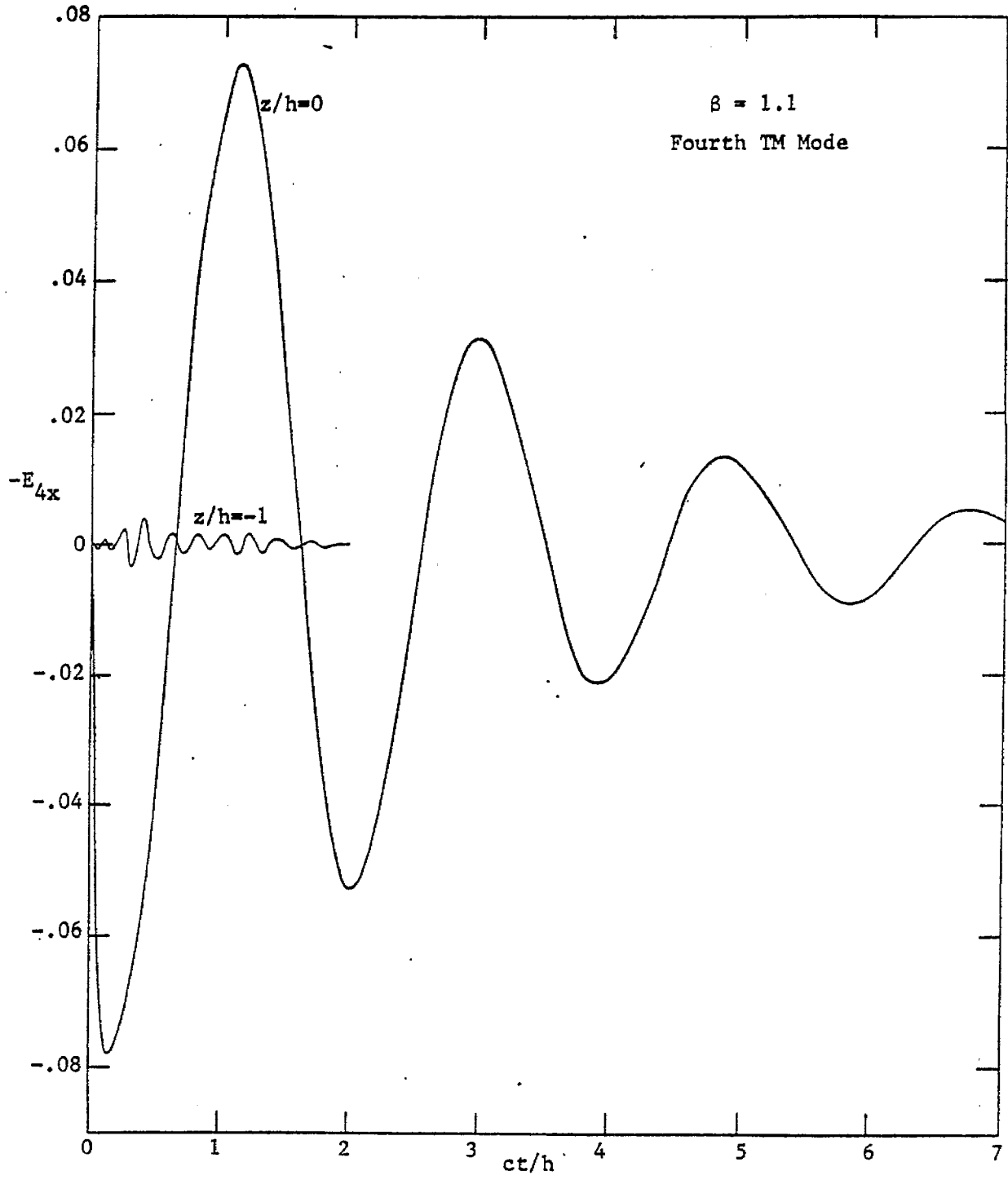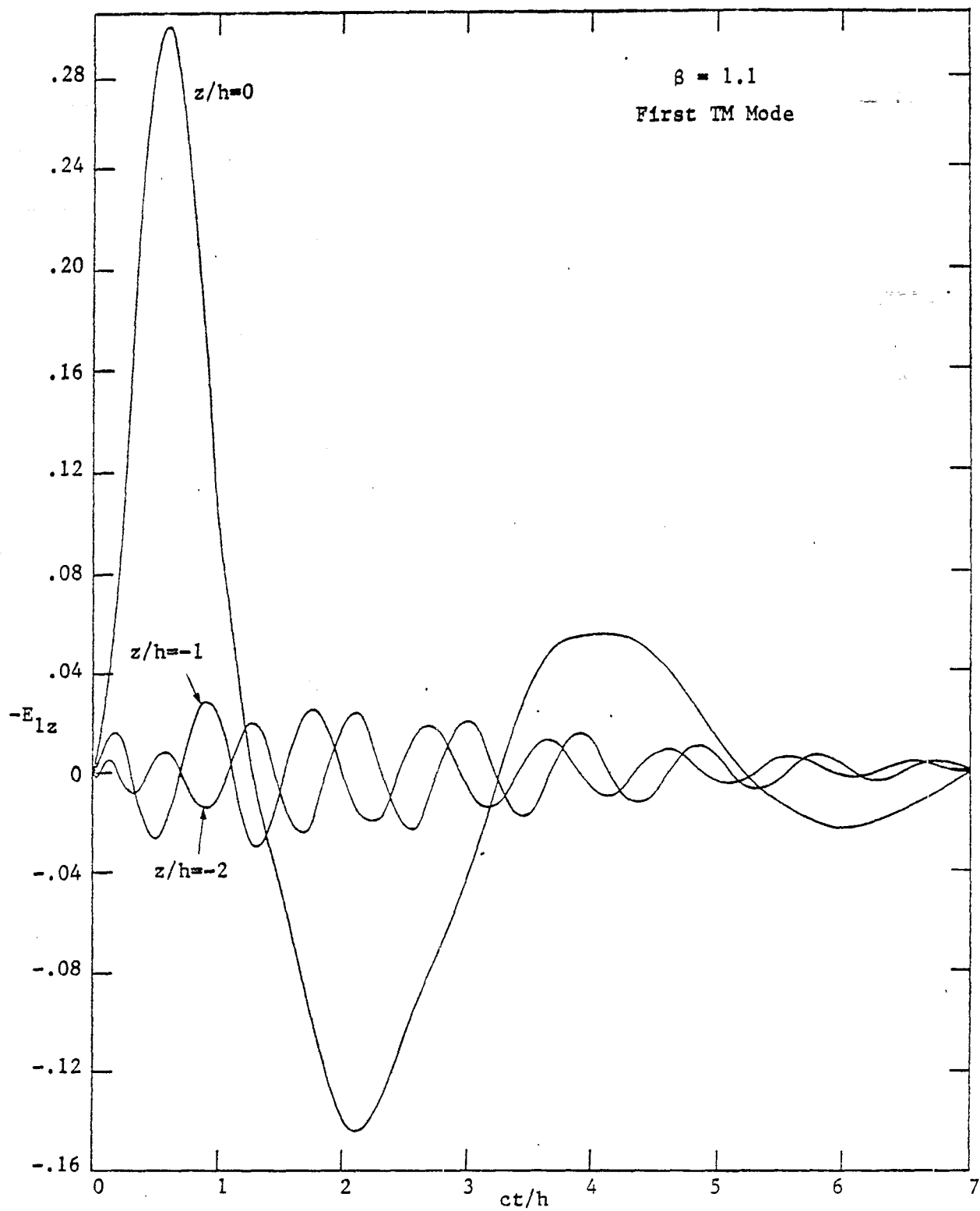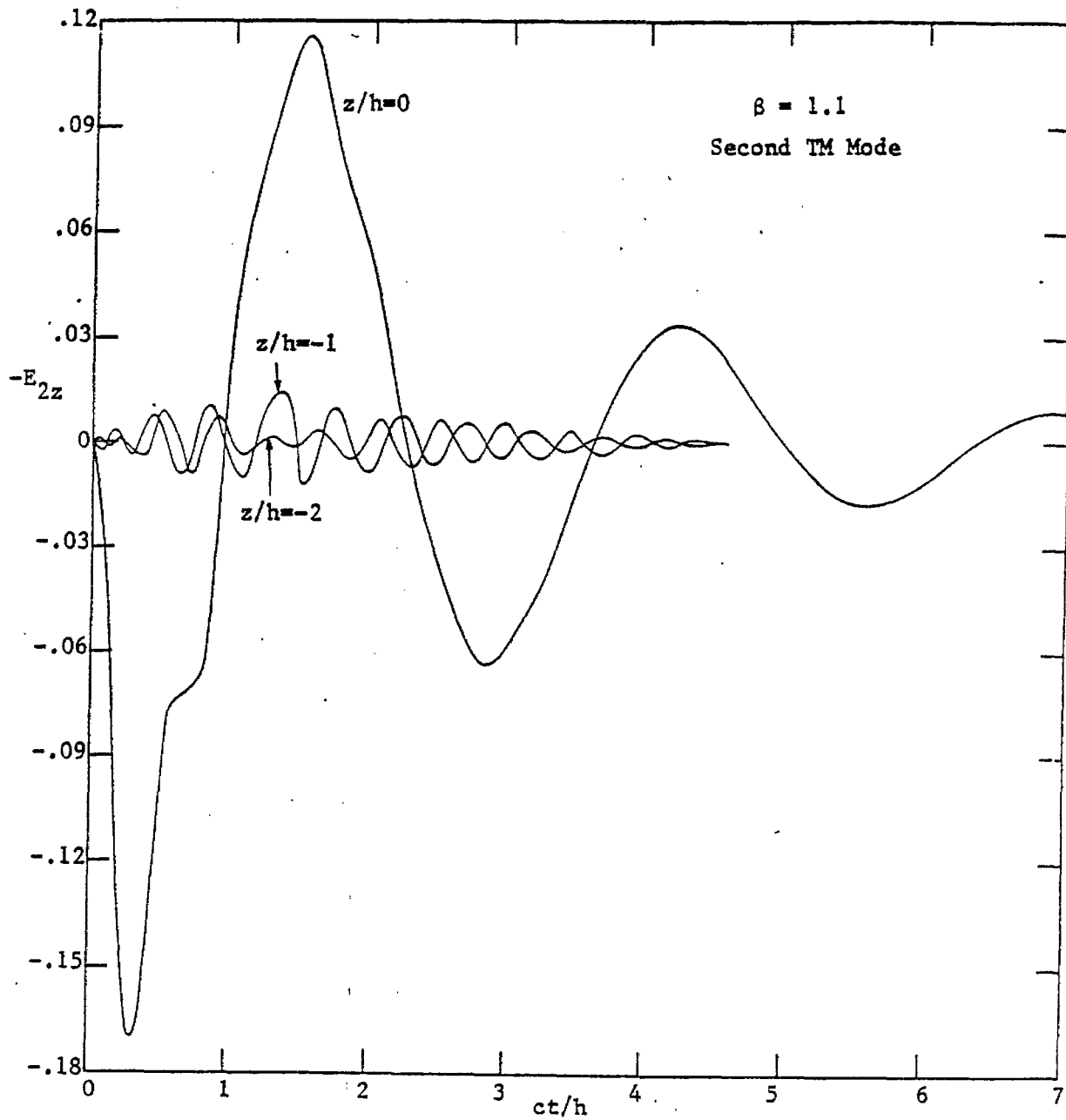
Figure 20

Figure 21
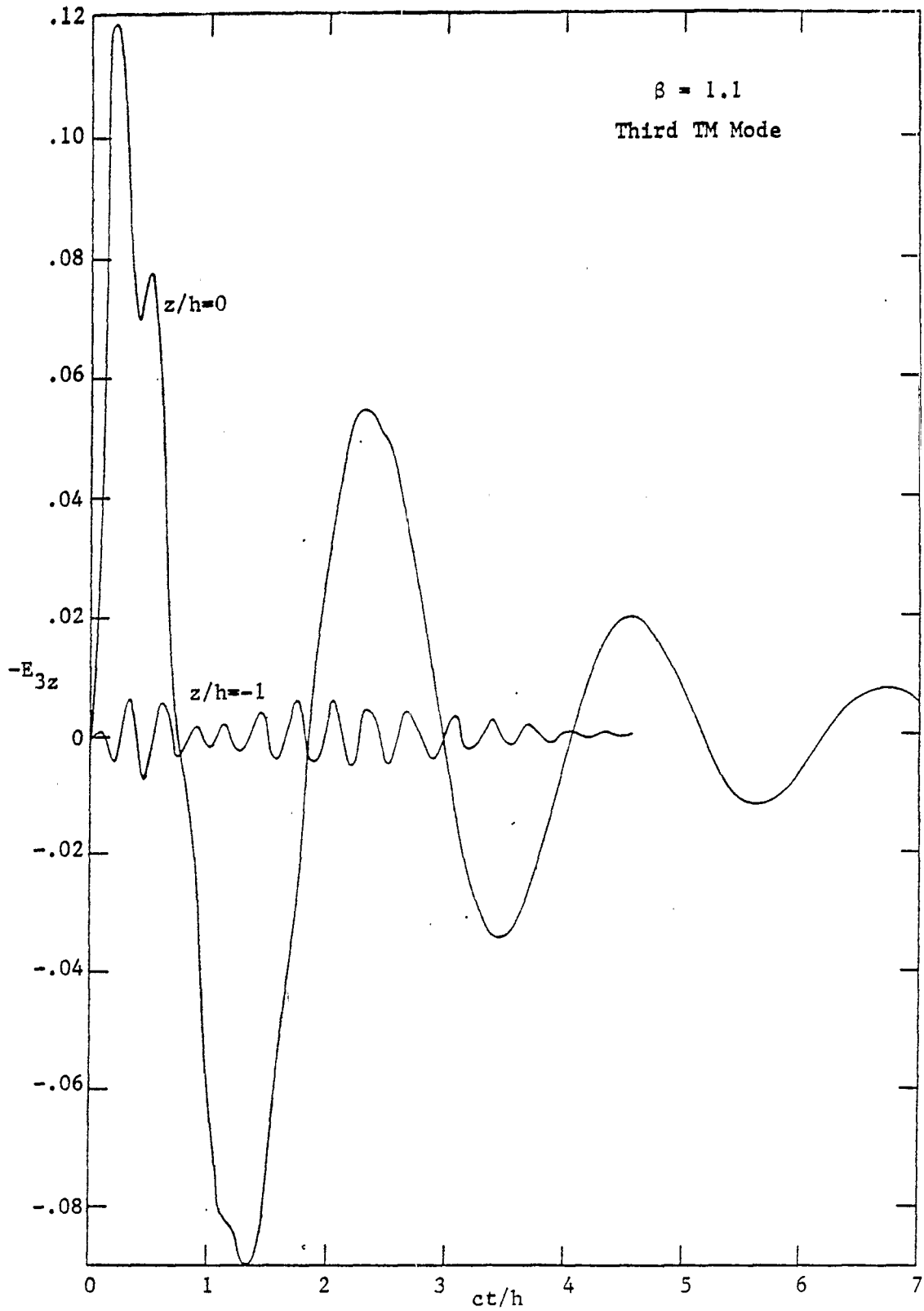
Figure 22
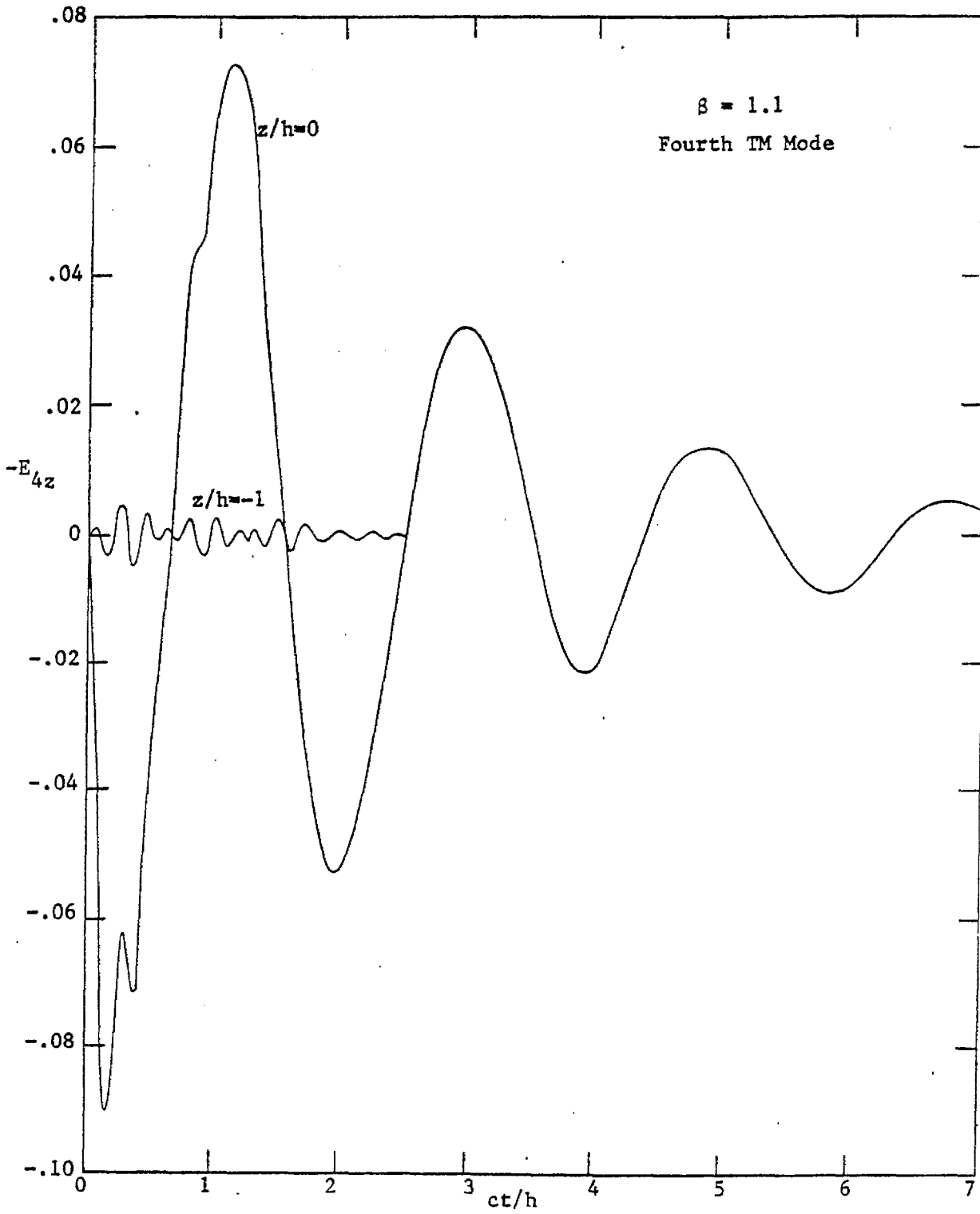
Figure 23

Figure 24

49
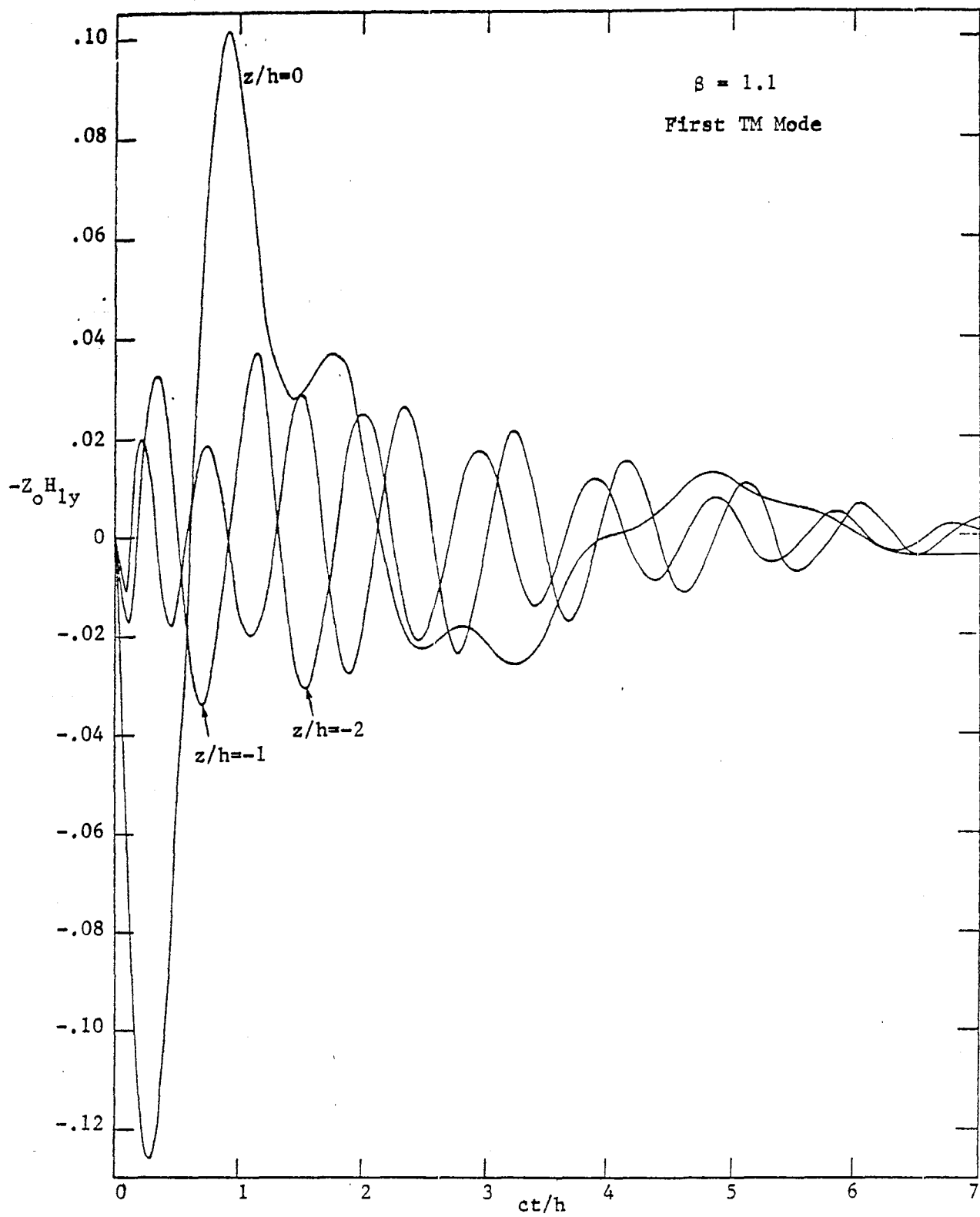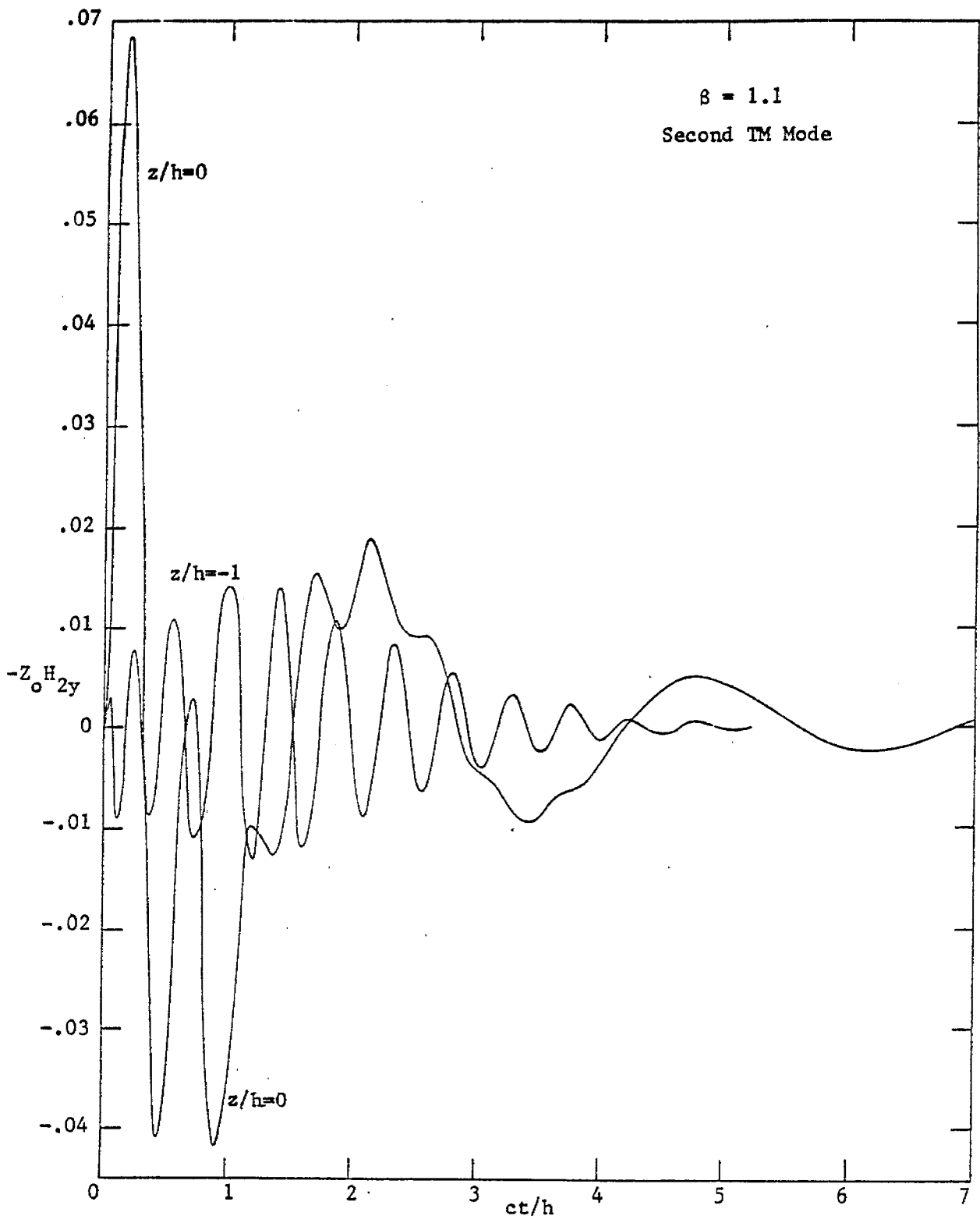
Figure 25

Figure 26
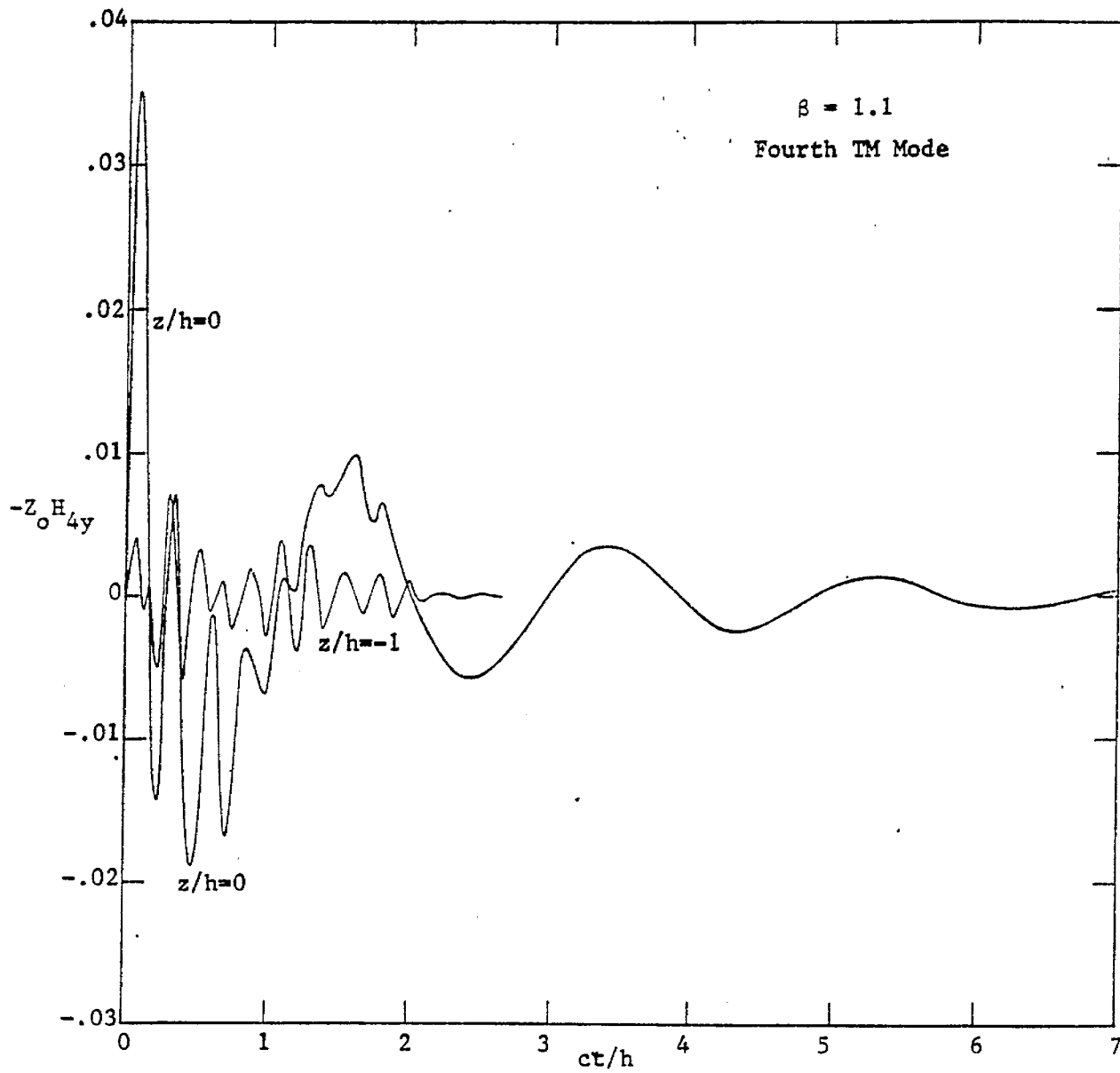
Figure 27

52

Acknowledgement

References

1. Carl E. Baum, "Admittance Sheets for Teminating High-Frequency Transmission Lines," Sensor and Simulation Note 53, April 1968.

2. Carl E. Baum, "A Sloped Admittance Sheet Plus Coplanar Conducting Flanges as a Matched Termination of a Two-Dimensional Parallel-Plate Transmission Line," Sensor and Simulation Note 95, December 1969.